

“A clean rig is a happy rig”

University of Alberta

Energy Metabolism in the Hypertrophied Newborn Rabbit Heart

by

Virgilio Jorge de Jesus Cadete

A thesis submitted to the Faculty of Graduate Studies and Research
in partial fulfillment of the requirements for the degree of

Master of Science

Medical Sciences - Pediatrics

©Virgilio Jorge Jesus Cadete

Fall 2010

Edmonton, Alberta

Permission is hereby granted to the University of Alberta Libraries to reproduce single copies of this thesis and to lend or sell such copies for private, scholarly or scientific research purposes only. Where the thesis is converted to, or otherwise made available in digital form, the University of Alberta will advise potential users of the thesis of these terms.

The author reserves all other publication and other rights in association with the copyright in the thesis and, except as herein before provided, neither the thesis nor any substantial portion thereof may be printed or otherwise reproduced in any material form whatsoever without the author's prior written permission.

Examining Committee

Gary D Lopaschuk, Pediatrics

Jason RB Dyck, Pharmacology

Peter E Light, Pharmacology

Dedication

This thesis is dedicated to my beloved wife, to my parents without whom I have never reached this far. To my grand parents and my uncles whom I hope I made them proud wherever they are!

Abstract

The newborn heart possesses a higher tolerance to ischemia in comparison to adult hearts. Post-ischemic interventions that increase energy production are beneficial for recovery. These data suggest that the newborn heart holds on a very tight energetic plasticity and may not be capable to effectively respond to increases in energetic demand. Congenital heart defects can lead to the development of cardiac hypertrophy and often require surgical intervention.

Using an animal model of newborn hypertrophy and biventricular isolated working heart we confirm the metabolic profile of the newborn rabbit heart, in which fatty acid oxidation provides the vast majority of energy to the heart. Our findings show that when right ventricle load is added, the increasing energy requirements are met by increasing glucose oxidation rates.

Our data generated by the isolated biventricular working heart model further supports the concept of the newborn heart in a state of deficient energy reserve.

Acknowledgements

I would like to thank everyone that made this possible:

- To my beloved wife for believing when I doubted and doubting when I blindly believed;
- To my parents for always doing everything they could possibly do and sometimes what was almost impossible to help me get here and for always believing in me; to my sister and Pedro, to my beautiful Maria that always brings a smile to my face;
- To my family for being there all the way (Thanks Helena, Alcides, Paulo, Rui, Ze, Angela)
- To my Canadian family for making me feel like home when I had none, for letting me be part of the family (thanks Jose e Maria, Lidia, Celestino, Marco e Gabriela, Jose, Suzy, Noah, Sarah e Johna, Joao, Marisol e Johnatan);
- Thanks Cliff and Karalyn for all that friendship has to give; Welcome Alexa!
- Thanks Hernando, Juliana e Sylvia for all the wise words in the tough moments;
- Thanks Donna “Grandma” Beker for the patience to teach me how to perfuse and for all the advice on life;
- Thanks Marie-Jo for always worrying way before I left Portugal and for not stopping worrying until today;

- Thanks Tatsu for all the understanding and good humor, and all the hard work that made this project possible;
- Thanks to everyone in the Lopaschuk's Lab for the help, for the listening and for the refreshing coffee breaks;
- Thanks to all my friends that made my life in Edmonton so much better and entertaining. I don't dare to name you all because I don't want to forget anyone (Thank you Cabrita);

- Thanks to my committee members Dr Jason Dyck and Dr Peter Light for all the patience during those committee meetings and always trying to find a way to be helpful;
- Thanks to my supervisor Dr Gary Lopaschuk for believing in me and giving me a chance, for doubting me when I slacked and needed to doubt myself, and believing again when the time came;
- Thanks to Dr Greg Sawicki and Jolanta for giving me back the pleasure of trying to be a scientist

Table of Contents

1. INTRODUCTION.....	1
The newborn heart metabolism.....	2
1.1.1 Hormonal and dietary control.....	2
1.1.2 Molecular control.....	5
Hypertrophy.....	10
1.1.3 Hypertrophic Phenotype.....	11
1.1.4 Hypertrophy of the adult heart.....	13
1.1.5 Hypertrophy of the newborn heart.....	16
The energy reserve theory.....	19
Rationale and hypothesis.....	22
2. METHODS.....	34
Aorta-caval fistula in 7 day-old New Zealand albino white rabbits.....	34
Evaluation and determination of the presence of the aorta-caval fistula following surgery..	35
Isolated biventricular working heart perfusions.....	37
1.1.6 Pre-load curves.....	37
1.1.7 Heart perfusions.....	37
1.1.8 Perfusion conditions.....	38
1.1.9 Metabolic rates analysis.....	39
Statistical analysis.....	41
3. RESULTS.....	50
Pre-load curves.....	50
Cardiac physiology alterations due to an aorta-caval shunt.....	51
Biventricular working heart perfusions.....	51
4. DISCUSSION.....	66
5. FUTURE DIRECTIONS.....	78
6. LIMITATIONS.....	80
BIBLIOGRAPHY.....	83

List of Tables

Table 1 - Echocardiographic measurements.	58
Table 2 - Functional measurements.....	60

List of Figures

Figure 1.1 – Schematic representation of substrate availability and metabolic pathway relevance to overall energy production in the fetal cardiomyocyte.	27
Figure 1.2 - Schematic representation of substrate availability and metabolic pathway relevance to overall energy production in the newborn cardiomyocyte.	29
Figure 1.3 - Schematic representation of substrate availability and metabolic pathway relevance to overall energy production in the adult cardiomyocyte.	31
Figure 1.4 – Contribution of different energy producing pathways to overall cardiac energy production (adapted from Lopaschuk et al., 1992).....	32
Figure 2.1 - Representative picture of a retroperitoneal incision performed on a 7 day-old rabbit.....	42
Figure 2.2 - Aorta-caval fistula. Schematic of the procedure performed to produce an aorta-caval fistula on a 7 day-old rabbit.....	45
Figure 2.3 - Color Doppler. Representative frame of shunt flow viewed by color Doppler.....	46
Figure 2.4 - The isolated biventricular heart. Schematic of the isolated biventricular working heart.....	47
Figure 2.5 - Schematic representation of the perfusion protocol for the isolated biventricular working heart perfusions.....	48
Figure 3.1 - Pre-load curves.....	57
Figure 3.2 - Steady state metabolic rates.....	62

Figure 3.3 - Steady state ATP production.60

Abbreviations

ACC	acetyl-CoA carboxylase
ADP	adenosine diphosphate
AICAR	5-aminoimidazole-4-carboxamide 1- β -D-ribofuranoside
AMP	adenosine monophosphate
AMPK	5'-AMP activated protein kinase
AMPKK	5'-AMP activated protein kinase kinase
ANOVA	analysis of variance
ATP	adenosine triphosphate
BSA	bovine serum albumin
Ca ²⁺	calcium ion
CaMKK	calmodulin dependent kinase kinase
CAT	carnitine acetyltransferase
CO ₂	carbon dioxide
CoA	coenzyme A
CPT1/2	carnitine palmitoyl transferase 1/2
Cr	creatinine
DCA	dichloroacetate
DNA	deoxyribonucleic acid
EDTA	ethylenediaminetetraacetic acid
FAD/FADH ₂	flavin adenine dinucleotide
FABP	fatty acid binding protein
FAT/CD36	fatty acid translocase
FATP	fatty acid transport protein
GAPDH	glyceraldehyde 3-phosphate dehydrogenase
GLUT	glucose transporter
GPT	glutamate-pyruvate transaminase
GTP	guanosine triphosphate
H ⁺	proton
HIF-1 α	hypoxia inducible factor-1 α
HR	heart rate
I/R	ischemia/reperfusion
LV	left ventricle
LVID	left ventricular internal diameter
LVWT	left ventricular wall thickness
MCD	malonyl-CoA decarboxylase
Na ⁺	sodium ion
NAD ⁺ /NADH	nicotinamide adenine dinucleotide
NADP/NADPH ₂	nicotinamide adenine dinucleotide phosphate
O ₂	oxygen
PDH	pyruvate dehydrogenase
PDK	pyruvate dehydrogenase kinase
PFK-1/2	phosphofructokinase-1/2

PSP
ROS
SEM
TCA
TG

peak systolic pressure
reactive oxygen species
standard error of the mean
tricarboxylic acid cycle
triglyceride

1. Introduction

The adult heart is an omnivorous organ capable of metabolizing a variety of substrates in order to meet its high energetic demand. Fatty acid oxidation (FOx) contributes with 60-90% of the ATP requirement of the adult heart, with the remaining being provided mainly by carbohydrate oxidation, including glucose and lactate oxidation. A much smaller contribution to energy metabolism is provided by glycolysis, ketone bodies and amino acid oxidation (Stanley, Recchia et al. 2005). Certain pathological conditions (such as diabetes, hypertension) disturb the normal physiology of the heart producing a compensated hypertrophy, which consists of elongation and enlargement of the cardiac myocyte to compensate for the increased workload. In a chronic setting the myocyte loses its capability to compensate for the increased workload and begins to fail (reviewed by (Heineke and Molkentin 2006). Decompensated hypertrophy is also associated with metabolic changes, which are consistent with the re-establishment of a fetal-like gene profile.

During the fetal period, the metabolic profile exhibited by the heart is limited by substrate available. Substrate availability is determined by the levels present in maternal blood and by the placenta. The placenta is a primary source of lactate and fairly impermeable to fatty acids. Glucose homeostasis mirrors that of the maternal blood. With birth, a dramatic change in substrate availability occurs with the beginning of suckling. In contrast to the mature adult heart, the newborn heart exhibits a very different metabolic profile, as it lacks the required

intracellular machinery to efficiently oxidize glucose, and the supply of substrates to the heart is limited by what is provided by the mother's milk (sole source of nutrients in the newborn diet). Substrate availability, in turn, conditions the hormonal profile in the blood stream, such as the circulating levels of insulin and glucagon. Hence, the newborn heart relies mainly on fatty acid oxidation (~50%), with lactate oxidation and glycolysis providing the vast majority of the remaining energetic requirements. During this very important period in the maturation of cardiac metabolism any insult that disturbs the normal physiology of the heart results in drastic consequences to cardiac development and may be life threatening. Indeed, more than 10% of human newborns express some form of congenital heart defect and eventually develop cardiac hypertrophy. Of those, approximately 30% have to undergo invasive corrective surgery (Hoffman 1995; Hoffman 1995). It is therefore very important to determine the effect of cardiac hypertrophy on metabolism and on the metabolic maturation undergoing during the newborn period, to develop potential therapeutic approaches.

The newborn heart metabolism

1.1.1 Hormonal and dietary control

Birth is a stressful event for every mammal. Almost immediately with birth the lungs start to function and blood oxygen supply is maintained at the expense of pulmonary function and no longer provided by maternal circulation.

This intense event results in a dramatic increase in circulating catecholamines (adrenaline and noradrenaline). Catecholamines are strong stimulators of glucagon release into the blood stream. Glucagon, often referred to as insulin's antagonist, stimulates the release of glucose to the blood stream by the liver. In peripheral tissues it inhibits glucose metabolism, stimulating, in turn, fatty acid metabolism.

The normal adult heart maintains contractile function and intracellular pathways (such as ion homeostasis, protein production, energy reserve production) at the expense of ATP hydrolysis. The great majority of ATP is generated in the mitochondria via oxidative phosphorylation, with β -oxidation of fatty acids providing the majority of acetyl-CoA (60-90%). Oxidation of carbohydrates (such as glucose/pyruvate and lactate) provides the remaining ATP, with glycolysis contributing less than 2% for total ATP production.

The fetal and newborn hearts however, due to a very different environment and very peculiar conditions present a very distinct metabolic profile. During the fetal period the availability of substrates presented to the heart for energy production is limited by the placenta. The fetal diet consists of predominantly carbohydrates (>60%), with the remaining 30-35% being mainly protein and fat (<10%) (Girard, Ferre et al. 1992). The placenta is fairly impermeable to free fatty acids resulting in a reduced supply of this substrate to the heart (fetal plasma concentration of free fatty acids <0.1mM). In addition, more likely due to the reduced supply and high rate of cell division and growth, the free fatty acids that cross the placenta are tunneled preferentially for cell

synthesis and storage in the liver and adipose tissue (Girard, Ferre et al. 1992). Consequently, oxidation of fatty acids in the fetal heart is a less important source of ATP than in the adult heart. Indeed, when 1-day old rabbit hearts (believed to exhibit a fetal metabolic profile) were perfused in the presence of high fat, fatty acid oxidation only contributed 13% of the total ATP generated (Lopaschuk and Spafford 1990)(Figure 1 and 4). This inability to oxidize free fatty acids by 1-day old rabbit hearts has been attributed to the mitochondrial inhibition of fatty acid uptake (Lopaschuk and Spafford 1990).

Lactate is actively produced by the placenta and represents the main substrate oxidized by the fetal heart. Glucose supply to the heart does not vary during the fetal period, reflecting the maternal plasma glucose levels. High rates of glycolysis, anaerobic glucose metabolism, occur during the fetal period due to limited oxygen supply, together with an immature oxidative pathway for glucose (Figure 1 and 4).

With birth, the newborn is exposed to a whole new environment with dramatic hormonal and dietary changes, which influence the metabolic profile of the heart. Birth is associated with a hormonal program that may trigger the release of stress hormones such as adrenaline and noradrenaline. These catecholamines are strong stimulators of glucagon release and inhibitors of insulin secretion. Stress induction due to cold exposure after birth or, primarily, cord cutting have been described as the physical events that lead to catecholamines secretion and the consequent drop in circulating levels of insulin and rise in glucagon seen in the early newborn period (Girard, Ferre et al. 1992).

Despite the important hormonal-induced changes in newborn heart metabolism, the major metabolic changes occur with the beginning of suckling. The maternal milk provides the newborn with the essential substrates for preservation of cell function and sustained growth. In contrast to adult and fetal, the newborn diet is mainly composed of fat. Although species differences can be observed, fat provides more than 50% of the energetic intake of the newborn, with the remainder coming from carbohydrates and proteins with variations between species (Girard, Ferre et al. 1992). The sustained high levels of plasma free fatty acids associated with low carbohydrates are essential in the maintenance of high plasma levels of glucagon and low plasma levels of insulin. In this scenario fatty acid oxidation becomes the most important source of ATP in the heart with the maturation of glucose oxidation not occurring until dietary changes associated with weaning occur (figure 2). Indeed, in rats weaned with a high-fat/low-carbohydrate diet plasma glucagon does not drop and insulin levels do not rise (Coupe, Perdereau et al. 1990). However, it remains to be elucidated if failure to increase plasma levels of insulin delays the full maturation of glucose oxidation. Although catecholamines are responsible for the initial rise in glucagon and drop in insulin plasma levels, the dietary restrictions are the key factor responsible for the hormonal maturation that usually occurs during weaning.

1.1.2 Molecular control

In addition to the hormonal- and dietary-induced changes in the regulation of cardiac energy metabolism, a number of intracellular molecular changes occur in response to both the hormone and dietary substrates. Several of these sites of regulation occur in the pathway of fatty acid β -oxidation. Fatty acid β -oxidation can be seen as a two-step process. The first step involves the transport of free fatty acids from the plasma through the cell membrane and into the mitochondria; the second step is the oxidation process itself that happens in the mitochondria and is subdivided into the β -oxidation cascade that oxidizes fatty acyl-CoAs to acetyl-CoA and the subsequent oxidation of acetyl-CoA by the tricarboxylic acid (TCA) cycle with production of reduced equivalents (NADH and FADH₂) that feed the oxidative phosphorylation pathway to produce ATP. The transport across the cardiomyocyte membrane is the first site of regulation in the adult heart. However, a few lines of evidence suggest that cellular membrane fatty acid transport does not constitute a limitation to the increase in fatty acid oxidation (Ducy, Pegorier et al. 1985) in the liver of newborns. This suggests that the mitochondrial transport of fatty acyl-CoAs is the major site of regulation of fatty acid oxidation in the newborn heart. Several studies have suggested and confirmed the involvement of the AMP-activated protein kinase (AMPK) and its regulation of malonyl-CoA production via acetyl-CoA carboxylase (ACC) (known as the AMPK-ACC-malonyl-CoA axis)(Lopaschuk and Spafford 1990; Itoi, Huang et al. 1993; Itoi and Lopaschuk 1993; Saddik, Gamble et al. 1993; Lopaschuk, Witters et al. 1994; Gamble and Lopaschuk 1997; Dyck, Barr et al. 1998; Kantor, Robertson et al. 1999). Malonyl-CoA is a potent endogenous

inhibitor of the enzyme carnitine-palmitoyltransferase I (CPT I) which is the rate limiting step of the transport of acetyl-CoA into the mitochondria. CPT I is located in the outer mitochondrial membrane and catalyzes the transfer of an acyl moiety from the cytosol to carnitine in the mitochondrial intramembrane space. The transport of long-chain acyl moieties from the cytosol to the mitochondrial matrix also requires the presence of carnitine/acylcarnitine translocase, which transports the acyl-carnitine across the inner mitochondrial membrane, and CPT II in the inner mitochondrial membrane, which reforms the acyl-CoA in the mitochondrial matrix. But it is at the level of CPT I (the rate limiting step in the process of mitochondrial fatty acid uptake) that malonyl-CoA acts. Malonyl-CoA is synthesized by carboxylation of acetyl-CoA catalyzed by ACC. When there is an abundance of energy within the cell (ATP) there is an increase in the acetyl-CoA/free CoA ratio. In these conditions acetyl-CoA is highly abundant and can be transported out of the mitochondria and carboxylated to malonyl-CoA, thus working on a feedback regulation of fatty acid β -oxidation by inhibiting uptake of fatty acids, hence fatty acid β -oxidation itself. Since accumulation of acetyl-CoA results from a favorable energetic status of the cell, it is beneficial to inhibit energy producing pathways and redirect substrates towards storage. The turnover of malonyl-CoA is completed by the action of a decarboxylase – malonyl-CoA decarboxylase (MCD). The inhibition of energy producing pathways in a time of plenty is not simply and randomly determined by fluctuations in substrates and metabolic pathways intermediates, but certainly needs to be coupled with an energetic biosensor of the cell's energetic status in order for this energetic fine

tuning to take place. One of these biosensors and a key regulator of energy metabolism is AMPK. AMPK is a protein kinase sensitive to the energetic status of the cell via binding to AMP and ATP. When the cell becomes energy deficient the concentration of intracellular AMP increases. AMP binds to AMPK activating it allosterically (Hardie and Carling 1997; Hardie and Sakamoto 2006). When active, AMPK phosphorylates and/or interacts with downstream targets in order to shut down energy consuming processes and turning on energy producing ones. In this scenario, AMPK, when active, is capable of phosphorylating and inhibiting ACC. As a consequence, levels of malonyl-CoA drop and fatty acid oxidation rates increase to match energetic demands. Besides allosteric activation by AMP, AMPK is also susceptible to phosphorylation and activation by a number of identified upstream kinases AMPKKs, including LKB1 and CamKKs (α and β). These upstream kinases may be capable of sensing energy deficiency states and stress, communicating this information to AMPK. Phosphorylation by upstream kinases of the Thr 172 residue of AMPK results in an increase in kinase activity (Soltys, Kovacic et al. 2006). However, in conditions of low energy demand, ATP binds to AMPK and prevents the phosphorylation of the threonine residue. Another important mechanism of AMPK inhibition is triggered by insulin (Gamble and Lopaschuk 1997) and mediated by Akt (Kovacic, Soltys et al. 2003). Insulin is secreted after a carbohydrate-rich meal and triggers the mobilization of the insulin-sensitive glucose transporter GLUT-4 in various tissues. Insulin signals via a tyrosine kinase-type receptor, which dimerizes and autophosphorylates upon insulin binding of phosphatidyl-inositol-3-phosphate

kinase (PI3K) resulting in mobilization of GLUT4-rich vesicles to the sarcolemmal membrane (Calvani, Reda et al. 2000). In addition, activation of protein kinase B (PKB)/Akt also occurs. PKB/Akt phosphorylates and inhibits glycogen synthase kinase 3 (GSK3) resulting in increased glycogen synthase activity and increased synthesis of glycogen (Sugden, Fuller et al. 2008). Also, PKB/Akt phosphorylates and inactivates AMPK (Kovacic, Soltys et al. 2003). This results in increased ACC activity and elevated levels of malonyl-CoA and consequently the inhibition of acyl moieties transport into the mitochondria at the level of CPT-I and subsequent decrease in fatty acid β -oxidation rates.

During the newborn period, circulating insulin levels are >10-fold lower than what is seen in the fetal period, and >5-fold in comparison to the adult (Makinde, Kantor et al. 1998). These changes in circulating insulin levels are inversely correlated with AMPK activity. In fact, AMPK activity increases shortly after birth which results in a dramatic decrease in ACC activity with a subsequent drop in malonyl-CoA levels (Lopaschuk, Witters et al. 1994; Kantor, Robertson et al. 1999). Lopaschuk et al. (Lopaschuk, Witters et al. 1994) reported in New Zealand white rabbit hearts that the malonyl-CoA levels drop approximately 20% in the first week post-birth, but this decrease is even more marked by 6 weeks of age (~50%) and accompanied by a decrease in ACC activity to a similar extent.

In summary, the newborn heart presents a very unique metabolic profile, relying mainly on fatty acid oxidation for energy production. This happens due to several factors: 1) diet; 2) slow maturation of glucose oxidation; 3) low levels of

insulin and high levels of glucagon and 4) increased activity of the AMPK-ACC-malonyl-CoA axis.

Hypertrophy

Hypertrophy is the enlargement of an organ, tissue or cell. Cardiac ventricular hypertrophy is characterized by increased myocyte volume accompanied by changes in gene expression profiles and increased protein synthesis to support cell growth. Hyperplasia is the enlargement of an organ due to cell division, hence an increase in cell number is observed. Hyperplasia plays a major role during fetal life for cardiac development. However, during newborn and adult life hyperplasia does not account for cardiac development since cardiac myocytes fully differentiate, losing their division capabilities. Hypertrophy can be classified as physiological or pathological. Physiological hypertrophy occurs when the response of the cardiac tissue to the increase in workload results in a match between energy production and function, i.e., the heart is capable to operate the necessary structural and metabolic changes in order to sustain function independently of the degree of increase in workload. This is commonly called adaptive hypertrophy or compensated hypertrophy. This type of hypertrophy is commonly observed during growth and in high-performance athletes (Heineke and Molckentin 2006). Pathological hypertrophy can result from a severe increase in workload due to hypertension, hypoxia, pressure and volume overload (Schonekess, Allard et al. 1996; Abdel-aleem, St Louis et al. 1998; Iemitsu,

Miyauchi et al. 2001). Although the initial stages of hypertrophy are also seen as an adaptive process, the persistence of the stimuli results in an energetic overload and a consequent mismatch between function and energy production. Ultimately this mismatch results in heart failure. Several pieces of evidence have been collected during the last two decades and will be discussed below.

1.1.3 Hypertrophic Phenotype

Cardiac response to a sustained increase in workload triggers a number of responses at the genetic, proteomic and metabolic levels (Chien, Knowlton et al. 1991; Sadoshima and Izumo 1997; Yamazaki, Komuro et al. 1999; Esposito, Rapacciuolo et al. 2002). Also important is the morphological adaptation of the cardiac tissue to the changes in the physical properties of contraction.

During fetal life cardiac growth occurs both due to hyperplasia (increase in cell number) and hypertrophy (increase in cell type) (Porrello, Widdop et al. 2008). Shortly after birth, cardiac myocytes become terminally differentiated and cardiac growth is sustained at the expense of cellular hypertrophy, stimulated by increases in workload as body size increases. This type of cardiac hypertrophy is usually referred as physiological hypertrophy. Physiological hypertrophy can also occur due to athletic conditioning. Prolonged exposure to exercise training can result in an increase in cardiac mass and depending on the type of exercise the phenotype presented can be different (Lauschke and Maisch 2009). For instance,

running (a type of isotonic exercise) results in eccentric hypertrophy while isometric exercise such as weight lifting results in concentric hypertrophy.

Pathological eccentric hypertrophy develops in response to either diastolic or diastolic and systolic wall stress increase due to, for instance mitral regurgitation or mitral regurgitation and arteriovenous fistulas, respectively (Krenz and Robbins 2004). Eccentric hypertrophy is characterized by an overall increase in cardiomyocyte length without an increase in cross-sectional area. This adaptive mechanism (increase in cardiomyocytes length) occurs by the addition of new sarcomeres in series (Opie, Commerford et al. 2006).

Concentric hypertrophy can develop due to isometric exercise but also due to pressure overload (pulmonary hypertension, aortic valve stenosis, among others). In contrast to eccentric hypertrophy, concentric hypertrophy occurs due to the addition of new sarcomeres in parallel and consequent increase in cardiomyocyte cross-sectional area (Opie, Commerford et al. 2006).

Another important feature of pathological hypertrophic growth is coronary reserve. Coronary reserve can be defined as the capability of the coronary circulation to increase its flow in order to meet increases in circulatory demand (oxygen and substrate supply). In concentric hypertrophy the ratio of capillary to cardiomyocytes remains unaltered, hence resulting in an increase in diffusion distance for nutrients and oxygen (Bache 1988; Isoyama, Ito et al. 1989). If sustained demand remains, the adaptive response will be vasodilatation of the coronary vasculature in order to increase supply to the cardiac tissue. A sustained status of coronary vasodilation reduces the potential of the vasculature to further

dilate in response to a sudden increase in demand. Hence, the hypertrophic heart is at a state of decreased coronary reserve.

1.1.4 Hypertrophy of the adult heart

The development of chronic pathological hypertrophy in adults ultimately leads to heart failure. This event is always preceded by gene transcription and translation changes alongside with metabolic profile changes (Lorell and Grossman 1987; Allard, Schonekess et al. 1994; Schonekess, Allard et al. 1997; Wambolt, Henning et al. 1999; Allard, Wambolt et al. 2000; Razeghi, Young et al. 2001; Sambandam, Lopaschuk et al. 2002). During the early stages of hypertrophic response (adaptive or compensated hypertrophy) the contribution of the several energy-producing pathways remains somehow unaltered with fatty acid β -oxidation still being the predominant pathway contributing to ATP production. However, in the chronic setting, fatty acid oxidation and related gene transcription is decreased with glycolysis and glucose oxidation becoming the major energy producing processes (Schonekess, Allard et al. 1996; Allard, Wambolt et al. 2000; Wambolt, Lopaschuk et al. 2000; Miyazaki, Oka et al. 2006). One way to interpret these findings is by examining the structure of the hypertrophied heart. The first stages of hypertrophic growth occur in order to compensate for the increased workload. To a certain extent perfusion of the growing myocardium muscle is adequate and matches energy and oxygen demands. When growth is no longer matched by angiogenesis and the increase in

diffusion time can no longer be compensated by vasodilation of the coronaries there is inadequate perfusion of the myocardium and the muscle becomes hypoxic (Shiojima, Sato et al. 2005; Walsh 2006). The oxygen is directed towards more efficient pathways (glucose oxidation), away from less efficient ones (fatty acid β -oxidation). Since glucose oxidation cannot provide enough energy for the maintenance of contractile function, glycolysis is also increased to match the energetic demands (Schonekess, Allard et al. 1996; Allard, Wambolt et al. 2000; Wambolt, Lopaschuk et al. 2000). These changes in the metabolic profile are accompanied by gene transcription changes. Indeed, to support the increasing glucose oxidation and glycolytic rates, genes associated with regulatory enzymes and/or proteins in both pathways exhibit increased transcription. Of particular interest is the decreased expression of proteins involved in fatty acid transport and binding (FAT/CD36 and FABP) (van der Vusse, van Bilsen et al. 2000). Importantly, defects in genes associated with fatty acid transport or binding have been related with the development of cardiac hypertrophy not only in rodents (spontaneously hypertensive rats) but also in humans (Tanaka, Okamoto et al. 1997; Tanaka, Sohmiya et al. 1997; Aitman, Glazier et al. 1999). Remaining to be elucidated, however, is the order by which these events occur: is the reduction in fatty acid transport proteins a consequence of reduced oxidative rates or the cause of the impaired rates of fatty acid β -oxidation?

In addition to the adaptive changes in proteins involved in transport of substrates, many other proteins are modified, including key regulatory enzymes involved in the regulation of metabolism, and contractile proteins. At this level,

the previously mentioned AMPK-ACC-malonyl CoA axis plays an important role in metabolic regulation. Kantor et al. (Kantor, Robertson et al. 1999) have shown in a model of newborn hypertrophy in piglet hearts that hypertrophy results in a decrease AMPK activity. This is associated with higher ACC activity and consequently higher levels of malonyl-CoA that result in an inhibition of fatty acid β -oxidation. An interesting observation is the decrease in the activity of the peroxisome proliferator-activated receptor alpha (PPAR α /NR1C1) in hypertrophied hearts (Young, Patil et al. 2001). PPAR α is a member of the nuclear receptor family and is a ligand-activated transcription factor. Known endogenous activators of PPAR α are long-chain polyunsaturated fatty acids, eicosanoids and prostaglandins D1 and D2. PPAR α has been extensively studied and among the PPAR family is the most well described receptor. PPAR α acts as a transcription factor by binding to specific sequences in the gene (known as peroxisome proliferators response elements, PPREs) and activating transcription. PPAR actions require mandatory heteromerization with co-factors such as PGC-1 α (peroxisome proliferators-activated receptor gamma co-activator 1 alpha) and the retinoid X receptor (RXR) (Smeets, Planavila et al. 2007). Of particular importance is the action of PPAR α in regulating fatty acid oxidation at various points in the pathway. Indeed, the genes expressing CPT-I and CPT-II, medium-chain acyl-CoA dehydrogenase and long-chain acyl-CoA synthetase have all been reported to possess PPREs in the promoter region (Mandard, Muller et al. 2004; Mandard, Zandbergen et al. 2004). Intriguingly, other genes have been reported to

respond to PPAR α activation, although they do not have PPRE, thus the mechanism remains to be elucidated. Among such genes are the ones encoding the cytoplasmic and the mitochondrial acyl-CoA thioesterases, MCD, uncoupling proteins 2 and 3 (UCP-2, -3) and pyruvate dehydrogenase kinase-4 (PDK-4). Although the regulation of PPAR α as a ligand-activated receptor and its role in the regulation of fatty acid oxidation are well established concepts, it has been recently described that PPAR α may be regulated by phosphorylation by a number of kinases including p38 MAPK, PKA and AMPK (Diradourian, Girard et al. 2005; Burns and Vanden Heuvel 2007). Activation of AMPK with AICAR resulted in increased levels of PPAR α mRNA with a concomitant increase in fatty acid oxidation. Moreover, inhibition of PPAR α and PGC-1 α prevented the AMPK-induced increase in fatty acid oxidation.

1.1.5 Hypertrophy of the newborn heart

The causes for hypertrophy during the newborn period are, most of the cases, distinct. Congenital heart disease is a fairly common event happening in ~8 out of every 1000 births (Hoffman 1995; Hoffman 1995). The causes for congenital heart disease can be due to patent fetal shunts or structural defects. In any case, the existence of a shunt between the right and the left heart (or the systemic and the venous circulations) results in increased return to the right ventricle and increased contractile work demand. To understand the

pathophysiology of congenital heart disease one must attend to the particularities of the fetal circulation. During fetal life the oxygen needed for the maintenance of aerobic pathways is provided by maternal blood *via* the placenta. This unique circulatory profile is maintained at the expense of physiologic shunts between venous and arterial circulation. Shunts are abnormal connections that allow blood to flow from one side of circulation to the other (Rhodes, Hijazi et al. 2008; Sommer, Hijazi et al. 2008; Sommer, Hijazi et al. 2008). The persistence of a shunt after birth will result in decreased circulatory efficiency, resulting in increased ventricular demand. The ductus arteriosus is a right-to-left shunt between the aorta and the main pulmonary artery. This shunt is essential in the fetus since it allows the blood from the right ventricle to bypass the lungs (non-functional in the fetus) and return to the maternal circulation via the descending aorta. The foramen ovale is also a right-to-left shunt. It is present in the fetal heart between the right and left atria (Sommer, Hijazi et al. 2008).

After birth the drastic changes in circulation and arterial pressures, together with hormonal stimuli lead to the closure of these shunts and establishment of circulation as is observed in the adult. However, if arterial pressure does not achieve a normal balance, these shunts may remain open increasing the work demand of the right ventricle resulting in pathological hypertrophic growth (Kantor, Robertson et al. 1999; Sommer, Hijazi et al. 2008).

Other causes of shunts are congenital heart defects. Atrial septa defects occur when the septum dividing the right and left atria does not form completely. After birth these defects result more frequently in left-to-right flow, and

consequently increased work demand of the right ventricle. Another type of malformation is the ventricular septa defect. In fact, this malformation is the most common, accounting for ~20% of all human cardiac malformations (Sommer, Hijazi et al. 2008). Ventricular septa defects can have several different origins but ultimately, as with patent shunts and atrial septa defects, result in increased flow to the right ventricle, increased workload and, ultimately, cardiac hypertrophy.

In the adult, as discussed above, it is well established that the hypertrophied heart exhibits dramatic changes at the molecular and metabolic levels. However, in the newborn heart, the effect of hypertrophy on metabolic and molecular profiles is not well studied.

Kantor et al. (Kantor, Robertson et al. 1999) provided important insight concerning the molecular changes happening in the newborn hypertrophied heart. In a model of volume overload due to a patent ductus arteriosus Kantor et al. demonstrates the involvement of the malonyl-CoA axis. During hypertrophy in the newborn heart there is a delay in the maturation of the activity of AMPK and ACC. This means that ACC activity remains high while AMPK remains low. The high activity of ACC is not due to changes at the transcriptional level but associated with post-translational changes. Indeed, the fact that AMPK activity remains low with the development of hypertrophy would lead to decrease phosphorylation of ACC and consequent increase in its activity. As mentioned previously, increased ACC activity results in increased levels of malonyl-CoA. The high levels of malonyl-CoA observed in the hypertrophied newborn heart suggest that significant inhibition of fatty acid β -oxidation must occur, shifting

metabolism towards glucose oxidation and glycolysis. In fact, Sheikh et al. (Sheikh, Barrett et al. 2009) in a model of RV hypertrophy reports increased protein levels of enolase. Moreover, the authors observe an increase in protein levels of medium chain acyl-CoA dehydrogenase. This observation further supports the inhibitory effect of malonyl-CoA on CPTI. This inhibition of the mitochondrial transport system for long-chain acyl-CoAs results in decreased rates of long-chain fatty acid β -oxidation. Due to the inhibition of this fulcrum energy-producing pathway, the newborn heart may adapt by improving its metabolic capability for medium-chain acyl-CoAs. Moreover, the β -chain of F₁-ATPase was also found to be downregulated as well as the heat shock 70 kDa protein 1 (HSP-70). HSP-70 is a protein involved in the translocation and assembly of the F₁-ATPase to the mitochondria. Taken together with the observations by Kantor et al. it appears that when a hypertrophic stimulus is applied to the newborn heart there is a delay in the maturation of key enzymes for metabolic regulation. Moreover, this delay in molecular maturation may result in a downregulation of the long-chain fatty acid β -oxidation pathway, which is compensated by an increase in enzymes related with glucose metabolism and medium-chain fatty acid β -oxidation. Nonetheless, the metabolic consequences of these changes at the molecular level remain to be elucidated.

The energy reserve theory

The capability to efficiently produce energy can be seen as the ability to tightly regulate rates of energy producing pathways and shift towards more efficient pathways under conditions of deprivation. In fact, the unique metabolic characteristics of the failing adult heart have been well studied (Stanley, Recchia et al. 2005) and been the focus of several interventions to optimize cardiac metabolism during heart failure. However, the metabolic implications of hypertrophy in the newborn heart are unknown.

As mentioned before, the newborn heart is surrounded by a unique and fast changing environment, associated to an extraordinary demand for energy production due to increased workload and growth. In order to meet the energy requirements for growth and function, the newborn heart relies highly on fatty acid β -oxidation. As discussed, after birth two events condition the contribution of glucose oxidation to energy production in the newborn heart: the dramatic drop in circulating levels of insulin and the low levels of carbohydrates in the newborn diet. For these reasons it is believed that glucose oxidation remains immature (or at least latent) until the beginning of weaning.

In the adult heart, after an ischemic episode, levels of circulating fatty acids dramatically increase and the reperfused adult heart relies on fatty acid oxidation for energy production (Stanley and Chandler 2002; Stanley, Recchia et al. 2005). This increased reliance on fatty acid β -oxidation has been associated with a worsening of recovery. In fact, increased reliance on fatty acid β -oxidation during early reperfusion will result in a high degree of uncoupling between glycolysis and glucose oxidation. The mechanism for the sustained uncoupling of

glucose metabolism during early reperfusion can be understood by referring to the glucose fatty acid cycle, also known as the Randle cycle (Randle, Garland et al. 1963). Under physiological conditions energy production to meet the energetic requirements is obtained by a fine tuned balance between energy producing pathways. Glucose oxidation and fatty acid β -oxidation pathways crosstalk. When fatty acid β -oxidation rates increase (for example during early reperfusion) the resultant increase in acetyl-CoA levels to feed to the TCA cycle are capable to decrease glucose oxidation by inhibiting the PDH complex preventing pyruvate produced by the glycolytic pathway to enter the mitochondria and be further oxidized by the TCA cycle. Conversely, when glucose oxidation rates increase a similar inhibitory effect on fatty acid β -oxidation rates can be observed. Since at the end of ischemia rates of glycolysis are extremely high (and null glucose oxidation), the maintenance of this uncoupling will result in further proton production (derived from uncoupled glycolysis) and a slower recovery of intracellular pH. In the case of the newborn heart this is not necessarily so. Unpublished data from our laboratory (Ito et al.) shows that high levels of fatty acids at reperfusion does not decrease recovery of hearts from 7 day-old rabbits. Also, no effect on glucose oxidation and glycolytic rates was observed. Of the most importance, high fat perfusion after ischemia did not result in increased proton production. When compared to low fat reperfused hearts, total acetyl-CoA was higher in the group reperfused with high fat. Recently, Olson et al. demonstrated the contribution of anapleurotic pyruvate to overall metabolism in

the newborn heart. Moreover, it is evident that when pyruvate is added as a substrate during reperfusion there was increased recovery.

Taken together, these independent observations strongly suggest that the newborn heart may be under energetic imbalance. Indeed, newborn hearts have been reported to quickly deplete glycogen stores and ATP during ischemia (Wittnich, Belanger et al. 2007). These observations may be interpreted as a problem of energy reserve. Shortly after birth and with the beginning of suckling the newborn heart shifts its metabolic profile from fetal (supported by carbohydrate utilization) to predominantly β -oxidation of fatty acids. This, associated with immaturity of glucose oxidation and low availability of carbohydrates, provides the newborn heart with limited tools to respond efficiently to an increase in the energetic demand. Importantly, during the development of hypertrophy, in which supra-physiologic growth occurs, the newborn heart would not be capable to respond the energetic needs and enter failure faster than the adult heart. The concept of the energy reserve issue is of the highest importance in the newborn heart since congenital heart defects often result in the development of hypertrophy. Furthermore, knowing the effects of hypertrophy on the maturing newborn heart gains more importance due to the recurrent need for surgical intervention to correct congenital heart defects.

Rationale and hypothesis

Newborn cardioenergetics is, by itself, one of the most exciting areas of cardiovascular research. The complex and unique environment that surrounds the newborn heart gives rise to an elaborate scenario of hormonal, substrate and enzymatic regulation of energy production. In addition, the capacity of this elaborate scenario and extremely unique organ to adapt to a dramatic insult such as congenital heart defects is unknown and of extreme importance to develop a valid approach to treat the newborn heart.

The newborn period is characterized by dramatic changes at the hormonal and substrates. Furthermore, changes in the mechanic demand to the heart in order to prepare to adulthood are of the highest importance. This transitory period is characterized by a dramatic decrease in the levels of circulating insulin which coordinated with decreased viability of carbohydrates for energy production result in a decrease contribution of glucose oxidation to overall energy production. This fairly poor contribution of glucose oxidation is compensated by high levels of available free fatty acids and, consequently, high rates of fatty acid β -oxidation. This metabolic profile is further supported (or induces) by changes at the molecular level. The malonyl-CoA axis balances towards favoring fatty acid β -oxidation: low levels of malonyl-CoA, high levels of AMPK activity and consequently lower levels of ACC activity. Although high rates of fatty acid β -oxidation appear to provide the majority of the ATP production needed to satisfy the energetic demands, the energy producing pathways may be performing at the maximum of its capabilities, resulting in a dangerous state of energy reserve deficiency. Congenital heart defects, due to fetal malformations or inability to

neutralize vital shunts for fetal circulation, often lead to volume overload of the right ventricle. Volume overload dramatically increases contractile demand and can lead to ventricular hypertrophy. In animal models of newborn cardiac hypertrophy, changes at the molecular and transcriptional levels have been described. Cardiac hypertrophy in the newborn heart is characterized by high levels of malonyl-CoA, in turn associated with high ACC activity (Makinde, Kantor et al. 1998; Kantor, Robertson et al. 1999). High ACC activity is due to low phosphorylation by AMPK and not transcriptional changes. Concomitantly, changes at the transcriptional level demonstrate increased expression of genes coding for enzymes involved in glucose metabolism and decreased expression of enzymes linked with the mitochondrial energy production chain. Taken together, these observations suggest that newborn cardiac hypertrophy is characterized by changes in the metabolic profile.

We hypothesized that volume overload-induced cardiac hypertrophy will result in changes of the metabolic profile of the heart, namely an inhibition of fatty acid β -oxidation rates. We further postulated that the reduction in fatty acid β -oxidation rates may induce a state of energy starvation due to the immaturity of the glucose oxidation pathway.

In this study we used a model of newborn volume overload by shunting the subrenal aorta and inferior vena cava. Because this model results in primarily right ventricular volume overload and the contribution of the right ventricle to total heart mass is higher than observed in the adult we developed a model of

isolated biventricular working heart perfusion system to evaluate the effects of hypertrophy on right and left ventricles separately.

Figure 1.1

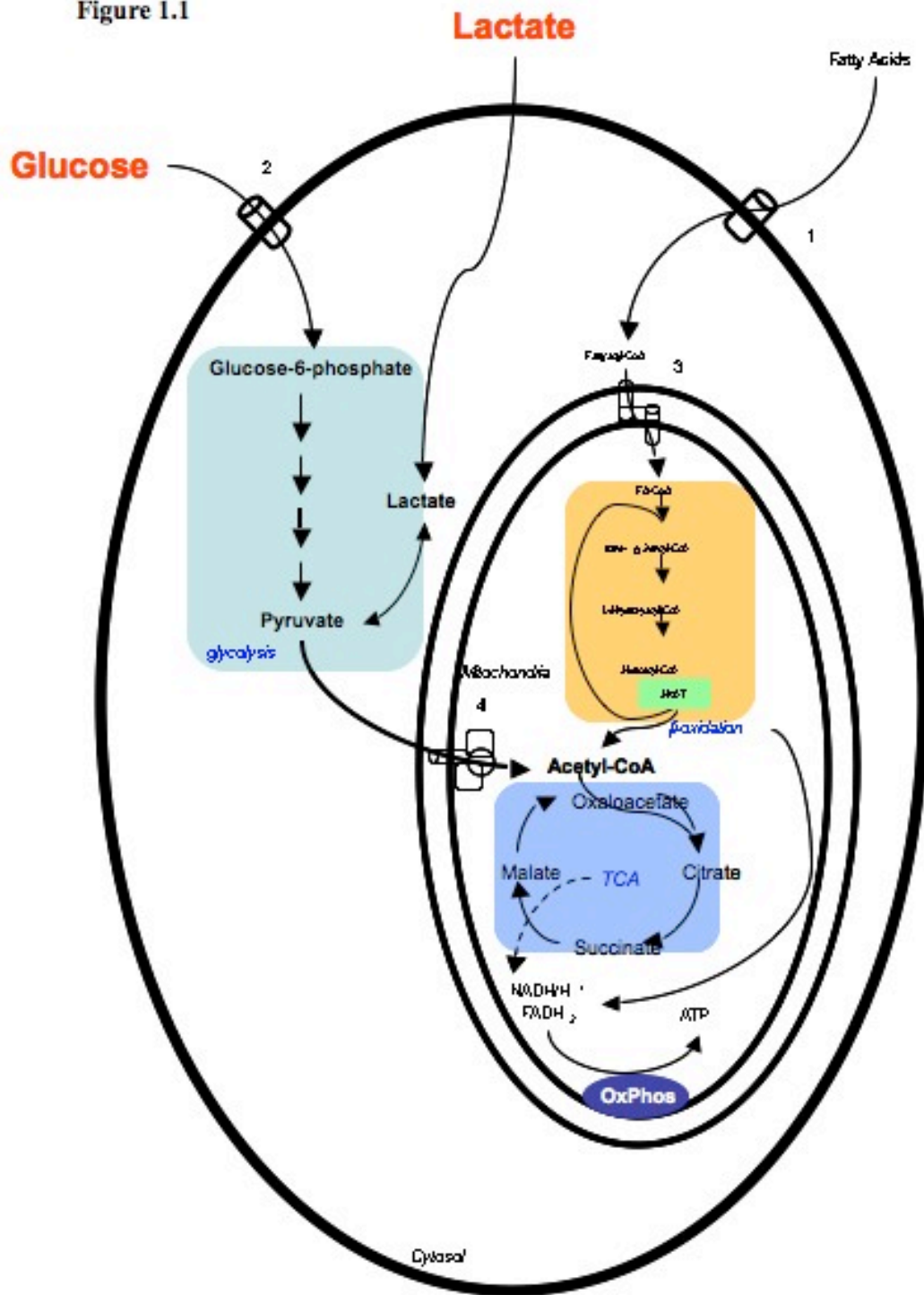


Figure 1.1 – Schematic representation of substrate availability and metabolic pathway relevance to overall energy production in the fetal cardiomyocyte.

During fetal life carbohydrate metabolism contributes with the majority of energy produced in the heart. Glucose and lactate (shown in red) are readily available substrates used by the cardiomyocyte to generate the energy (ATP) needed to maintain function and support growth. Fatty acids, are less available as an energy production substrate and contribute much less to overall cardiac energy production. Fatty acids are transported into the cytosol by a fatty acid transporter (1) FAT/CD36 and coupled with co-enzyme A. Entrance of fatty acyl-CoA into the mitochondria is mediated by the CPT1-CAT-CPT2 system (3). Once in the mitochondria fatty acyl-CoA is readily metabolized through the fatty acid β -oxidation pathway and the resultant acetyl-CoA directed to the tricarboxylic acid (TCA) cycle for production of reducing equivalents that feed the oxidative phosphorylation pathway (OxPhos) for ATP production. Glucose transport across the plasma membrane is mediated by glucose transporters GLUT1 (2). After phosphorylation by hexokinase to glucose-6-phosphate glucose is metabolized to pyruvate by the glycolytic pathway. Pyruvate is transported across the mitochondrial membrane and metabolized to acetyl-CoA by the pyruvate dehydrogenase complex (4). Once in the mitochondria acetyl-CoA enters the TCA cycle producing reducing equivalents that will then feed the OxPhos pathway and results in ATP production.

Figure 1.2

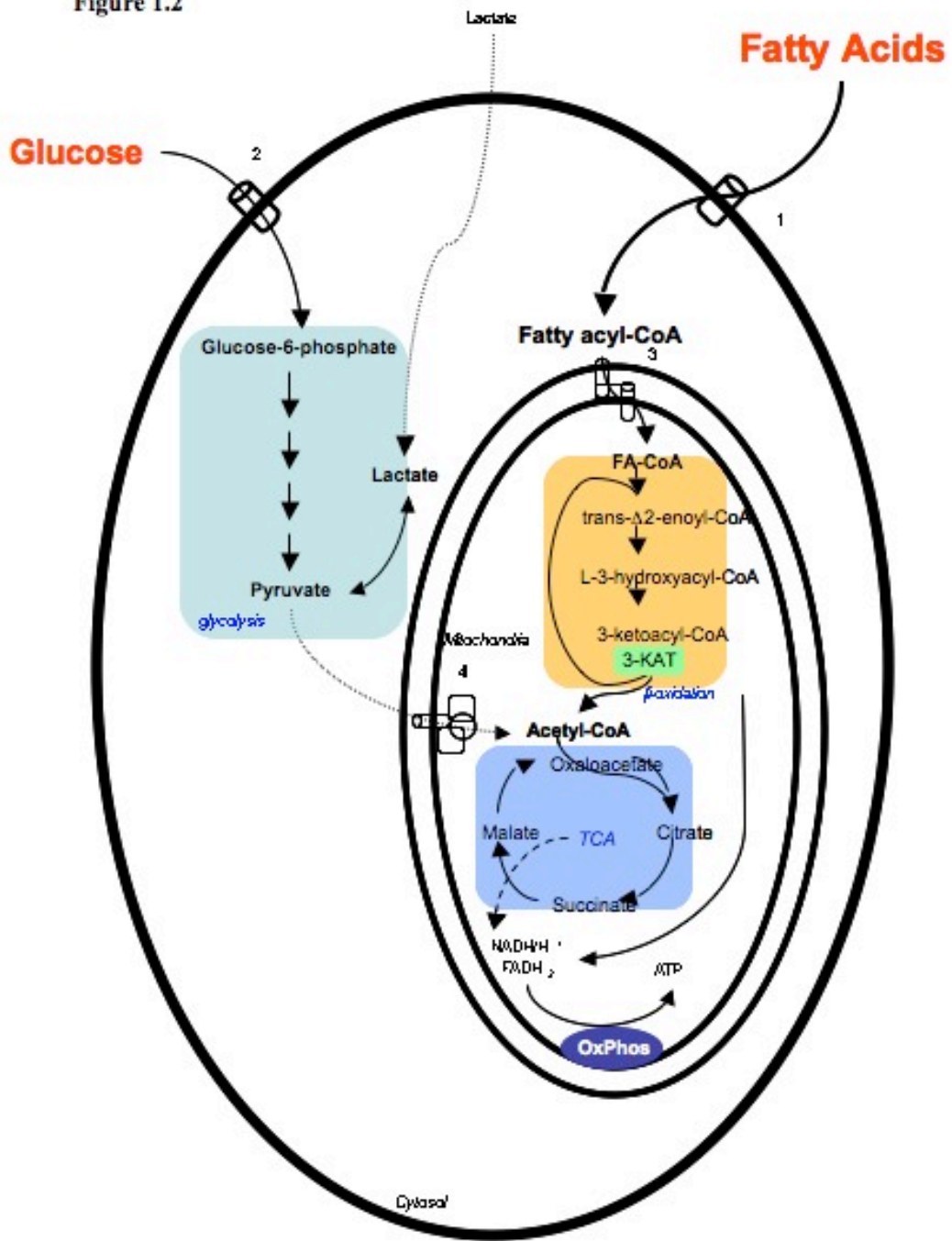


Figure 1.2 - Schematic representation of substrate availability and metabolic pathway relevance to overall energy production in the newborn cardiomyocyte. During the newborn period carbohydrate metabolism contribution to overall energy production dramatically drops. Fatty acids (in red) are the major substrate for energy production and contribute with the vast majority of cardiac energy production. Fatty acids are transported into the cytosol by a fatty acid transporter (1) FAT/CD36 and coupled with co-enzyme A. Entrance of fatty acyl-CoA into the mitochondria is mediated by the CPT1-CAT-CPT2 system (3). Once in the mitochondria fatty acyl-CoA is readily metabolized through the fatty acid β -oxidation pathway and the resultant acetyl-CoA directed to the tricarboxylic acid (TCA) cycle for production of reducing equivalents that feed the oxidative phosphorylation pathway (OxPhos) for ATP production. Glucose transport across the plasma membrane is mediated by glucose transporters GLUT1 (2). After phosphorylation by hexokinase to glucose-6-phosphate glucose is metabolized to pyruvate by the glycolytic pathway. Pyruvate is transported across the mitochondrial membrane and metabolized to acetyl-CoA by the pyruvate dehydrogenase complex (4). Once in the mitochondria acetyl-CoA enters the TCA cycle producing reducing equivalents that will then feed the OxPhos pathway and results in ATP production.

Figure 1.3

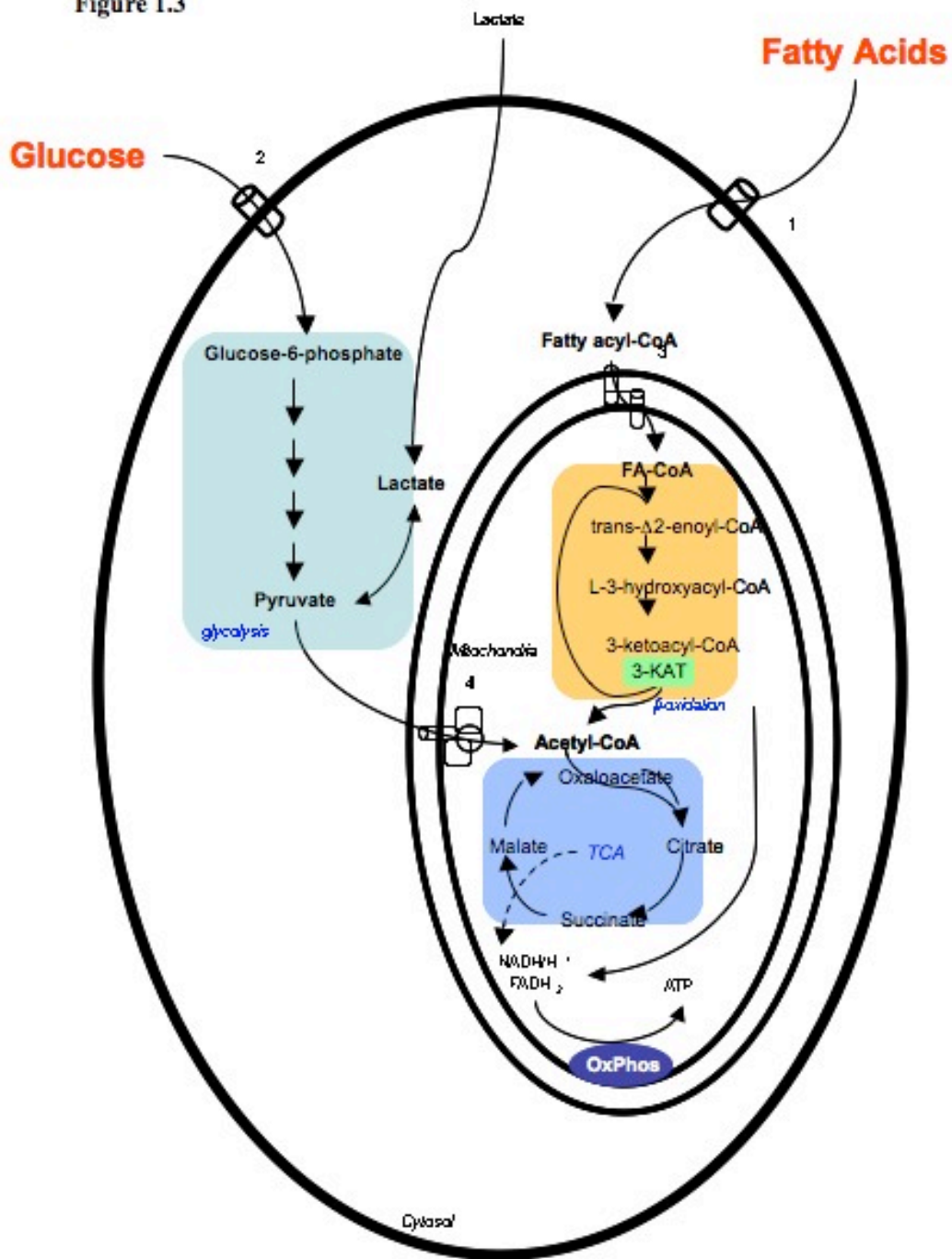


Figure 1.3 - Schematic representation of substrate availability and metabolic pathway relevance to overall energy production in the adult cardiomyocyte.

During adult life carbohydrates and fatty acids are present in the diet in abundance. Glucose and fatty acids become the major substrates for energy production and contribute with the vast majority of cardiac energy production. Fatty acids are transported into the cytosol by a fatty acid transporter (1) FAT/CD36 and coupled with co-enzyme A. Entrance of fatty acyl-CoA into the mitochondria is mediated by the CPT1-CAT-CPT2 system (3). Once in the mitochondria fatty acyl-CoA is readily metabolized through the fatty acid β -oxidation pathway and the resultant acetyl-CoA directed to the tricarboxylic acid (TCA) cycle for production of reducing equivalents that feed the oxidative phosphorylation pathway (OxPhos) for ATP production. Glucose transport across the plasma membrane is mediated by glucose transporters GLUT1 (2). After phosphorylation by hexokinase to glucose-6-phosphate glucose is metabolized to pyruvate by the glycolytic pathway. Pyruvate is transported across the mitochondrial membrane and metabolized to acetyl-CoA by the pyruvate dehydrogenase complex (4). Once in the mitochondria acetyl-CoA enters the TCA cycle producing reducing equivalents that will then feed the OxPhos pathway and results in ATP production.

Figure 1.4

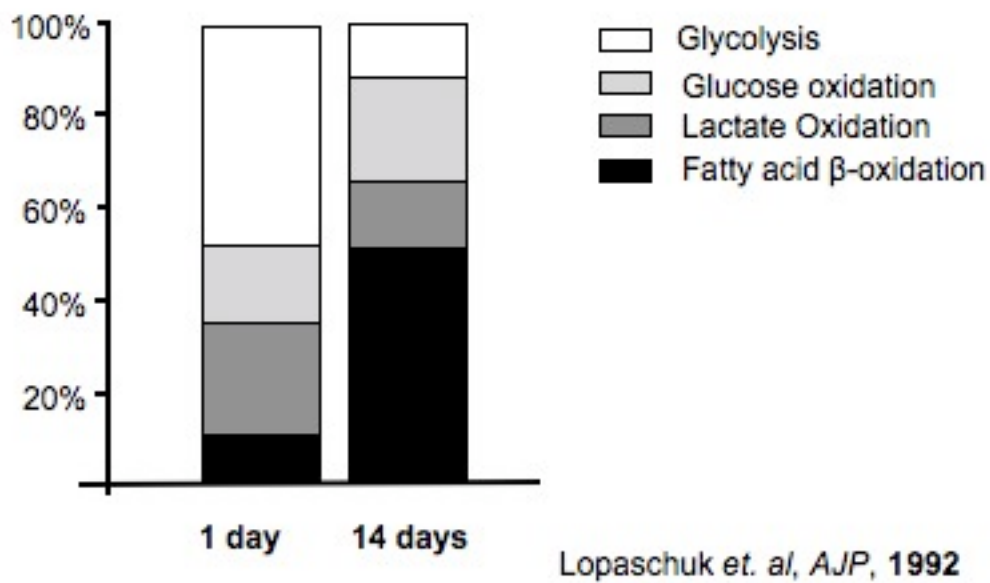


Figure 1.4 – Contribution of different energy producing pathways to overall cardiac energy production (adapted from Lopaschuk et al., 1992). Immediately after birth and before the beginning of suckling the circulating levels of substrates in the blood reflect those present during fetal life. Hence the 1 day-old heart exhibits a metabolic profile that is believed to reflect the fetal profile. In 1 day-old rabbit hearts glycolysis contributes with approximately 50% of overall

ATP production with the remaining being provided by lactate oxidation, glucose oxidation and fatty acid β -oxidation, in correspondent decreased order of contribution. By 14 days of age maternal milk is the sole source of energy provided in the newborn diet. The vast majority of energy provided by maternal milk is in the form of fatty acids with the remaining being provided by carbohydrates. In these conditions the 14 day-old rabbit heart relies on oxidation of fatty acids to produce almost 60% of its energetic requirements with the remaining being provided by glucose oxidation, lactate oxidation and glycolysis, in correspondent decreased order of contribution.

2. Methods

All animal experiments were performed accordingly to the guidelines from the Canadian Council on Animal Care and approved by the University of Alberta.

Aorta-caval fistula in 7 day-old New Zealand albino white rabbits

An aorta-caval fistula was produced in the sub-renal portions of the aorta and inferior vena cava (IVC). Seven day-old New Zealand albino white rabbits were removed from maternal care after their maternal milk intake and kept at room temperature as a litter while waiting for surgical procedure to be performed, as follows, in a clean but non-sterile environment.

Seven day-old rabbits were anesthetized by isoflurane inhalation (1-2%, oxygen flow rate of 2-3 ml/min). After achievement of surgical plane the animals were placed on a warming table at 37° C to maintain body temperature constant. The pups were placed on their right flank and the left flank shaved in order to expose the skin. Iodine solution (1%) was applied to assure aseptic conditions, followed by the injection of xylocaine (0.2 ml of a 1% solution) to eliminate any remaining pain reflex. A left flank retroperitoneal incision was performed and the sub renal portions of the aorta and IVC (inferior vena cava) (figure 2.1) exposed. An 18G needle with a 1½ length was modified by producing a 45° angle approximately 5 mm from the edge (figure 2.2). This modification allows easier puncturing of the aorta and IVC. Using the modified needle, the aorta was

punctured as well as the adjacent walls of the IVC and the aorta (figure 2.2). The aorta was then clamped upstream of the puncture site to avoid uncontrolled bleeding after needle removal. The needle was then carefully removed and a drop of “crazy glue” placed on the puncture site and let to dry. After drying of the glue the clamp was carefully removed and assurance of absence of bleeding was taken. The inner layers of peritoneum were sutured using stitch-by-stitch, as well as the skin incision. Isoflurane supplementation was then ceased and the rabbits let to recover in a warming table at 37° C and room air. The pups were monitored continuously for the following 2 hours, period after which they were re-introduced to the doe. Signs of rejection or distress were monitored for the following 6 hours. If successful recovery and re-introduction to the doe occurs the animals were kept for 14 days post surgery until the day of perfusion. Seven days post-surgery the animals returned for echocardiographic evaluation of the surgical procedure efficiency.

Evaluation and determination of the presence of the aorta-caval fistula following surgery

One week after surgery the rabbits returned for evaluation of the surgical procedure by echocardiography according to the American Society of Echocardiography (ASE) guidelines for echocardiographic assessment. The presence of an aorta-caval fistula was determined using color Doppler. A 15 MHz probe attached to an Acuson Sequoia C512 was used. In the presence of laminar

flow in two different directions, red coloring represents flow towards the transducer while blue coloring represents flow away from the transducer. When turbulent flow occurs there is the formation of a mosaic pattern. An aorta-caval fistula will result in local blood flow turbulence and can be determined by color Doppler (figure 2.3). The probe was placed over the fistula point and data acquired. Also IVC diameter was measured.

In the presence of an aorta-caval fistula there is an increase in blood return to the right ventricle resulting in morphological changes in the heart. In order to assess these modifications, 2 dimensional (2D) measurements were performed using 3 orthogonal planes of imaging as recommended by the ASE: long axis, short axis and four-chamber. Using these 3 planes we determined left ventricular end-diastolic volume (LVEDV), right ventricular area (RVA) and left ventricle (LV) wall thickness. A 17.5 MHz probe attached to the Visual Sonics Vevo 770 was used for 2D. These parameters allow the determination of the consequences of an aorta-caval shunt and also the degree of hypertrophic growth due to the surgical intervention.

Isolated biventricular working heart perfusions

1.1.6 Pre-load curves

Hearts from control (non submitted to surgery), sham and shunt animals were submitted to isolated biventricular working heart perfusion at different pre-loads to determine the conditions closer to what the 21 day-old rabbit hearts experiences *in vivo*. Our system is adapted from the one described by Itoi and Lopaschuk (Itoi and Lopaschuk 1993). In that study 14 day-old rabbit hearts were used. Since the 21 day-old rabbit heart is subjected to significantly higher pressure we decided to optimize perfusion conditions. Left and right ventricular pre-loads were always changed by increasing pre-load with time and independently from one another. Functional data was acquired after each pre-load jump and averaged for each pre-load from no least than 2 replicates.

1.1.7 Heart perfusions

On the day of perfusion the 21 day-old rabbits were removed from the doe after their matinal daily meal and hearts were perfused no later than 6 pm. The rabbits were anesthetized with sodium pentobarbital (60 mg/kg body weight). Once surgical plain was achieved a sternotomy was performed and the heart quickly excised and placed in cold Krebs-Henseleit (KH) buffer solution.

Within 30 seconds from excision of the heart the aorta was quickly isolated and cannulated and the heart retrogradely perfused using the Langendorff apparatus with KH buffer solution. The hearts were retrogradely perfused for 15 minutes, period during which the pulmonary artery (PA), the superior vena cava (SVC) and the left atria (LA) were isolated and cannulated. Also, the inferior vena cava (IVC) was isolated and occluded (Figure 2.4).

Left heart work was induced at the end of the 15-minute retrograde perfusion by initiating flow into the left atria while opening the aortic afterload line and terminating the retrograde perfusion. Right heart work was added by allowing flow into the right atria, through the SVC. Flow through the PA was never interrupted during the whole perfusion protocol. Figure 2.5 shows a schematic of the perfusion protocol.

1.1.8 Perfusion conditions

The KH buffer solution used for the retrograde perfusion system was prepared by adding glucose (5.5 mM) to a KH buffer ($[\text{Na}^+] = 133 \text{ mM}$, $[\text{K}^+] = 5.9 \text{ mM}$, $[\text{Cl}^-] = 127.7 \text{ mM}$, $[\text{Mg}^{2+}] = 1.2 \text{ mM}$, $[\text{H}_2\text{PO}_4^-] = 1.2 \text{ mM}$, $[\text{Ca}^{2+}] = 2.5 \text{ mM}$, $[\text{HCO}_3^-] = 25 \text{ mM}$) at pH 7.4. For the working heart perfusion apparatus, to the above KH solution palmitate (0.8 mM) was added after being pre-bound to 3% BSA and lactate (0.5 mM).

For metabolic rate measurements the hearts were perfused under the following preloads and afterloads: LA = 12 mmHg, RA = 11 mm Hg, Ao = 35 mmHg and PA = 4.5 mmHg.

1.1.9 Metabolic rates analysis

Glycolysis, glucose oxidation (GOx) and palmitate oxidation (POx) rates were measured by using trace amounts of radioactive labeled substrate in the perfusion buffer as described previously (Itoi and Lopaschuk 1993). Glycolytic rates were determined by measuring the accumulation of tritiated water ($^3\text{H}_2\text{O}$) resultant from tritiated glucose ($[5\text{-}^3\text{H}]\text{glucose}$) metabolization through the glycolytic pathway (at the level of Enolase). Buffer samples were collected at constant time points throughout the perfusion protocol and $^3\text{H}_2\text{O}$ extracted as described. Briefly, 200 μl of buffer were placed in a 1.5 ml microcentrifuge tube and incubated at 50°C for 24 hours inside of a sealed scintillation vial containing 500 μl of double distilled water. A $1\mu\text{Ci}/\mu\text{l}$ standard was also included to determine transfer efficiency. The vials were removed from incubation and condensation was reinforced overnight at 4°C . During these two incubations water from the buffer and the standard undergoes an evaporation-condensation cycle and transfers to the double distilled water. After the overnight incubation the microcentrifuge tubes were removed and discarded. Four milliliters of scintillation liquid is added to the scintillation vials and counted in a Beckman LS

3801 scintillation counter. Obtained decays per minute (dpm) counts were corrected for transfer efficiency and both cumulative and rate of production of $^3\text{H}_2\text{O}$ through time calculated taking into account that each mole of glucose metabolized by the glycolytic pathway results in the production of 1 mole of $^3\text{H}_2\text{O}$.

Glucose oxidation rates were determined using $[\text{U-}^{14}\text{C}]$ glucose as a radiotracer. The principle behind the determination of the metabolic rates lies on the decarboxylation steps of the tricarboxylic acid (TCA) cycle (Krebs cycle) catalyzed by isocitrate dehydrogenase and α -ketoglutarate dehydrogenase. After metabolization through the glycolytic pathway two molecules of $[\text{U-}^{14}\text{C}]$ pyruvate are produced from each molecule of $[\text{U-}^{14}\text{C}]$ glucose metabolized. Pyruvate can be further metabolized under aerobic conditions and feed into the TCA cycle when converted into $[\text{U-}^{14}\text{C}]$ acetyl-CoA by the pyruvate dehydrogenase complex (PDC). The $^{14}\text{CO}_2$ produced can either be in the gaseous form or in solution as bicarbonate ($\text{H}^{14}\text{CO}_3^-$). To account for these two sources of $^{14}\text{CO}_2$ buffer samples were collected at constant time points. One milliliter of buffer was added to 1 ml of 9 N H_2SO_4 . In the presence of a strong acid bicarbonate anions readily convert to CO_2 and water. This reaction was performed in a sealed system and the CO_2 produced trapped in hyamine hydroxide that is then counted in a Beckman LS 3801 scintillation counter for determination of the $^{14}\text{CO}_2$ fraction. The biventricular working heart perfusion system is also a sealed system. To determine the gaseous fraction of $^{14}\text{CO}_2$ produced an exit air line is immersed in 15 ml of hyamine hydroxide to trap all the exiting CO_2 . At the same time points

as the buffer sampling, hyamine sampling (300 μ l) was performed and counted for determination of the radioactive CO₂ fraction.

Palmitate oxidation rates were determined based on the same principles described above for glucose oxidation and [1-¹⁴C]palmitate was the radioisotope used.

Statistical analysis

Statistical analysis was performed using Microsoft Office Excell 2004 data analysis. One-way analysis of variance (ANOVA) yielding a p value lower than 0.05 was considered statistical significant. Number of replicates (n numbers) are mentioned in the figure legends.

Figure 2.1

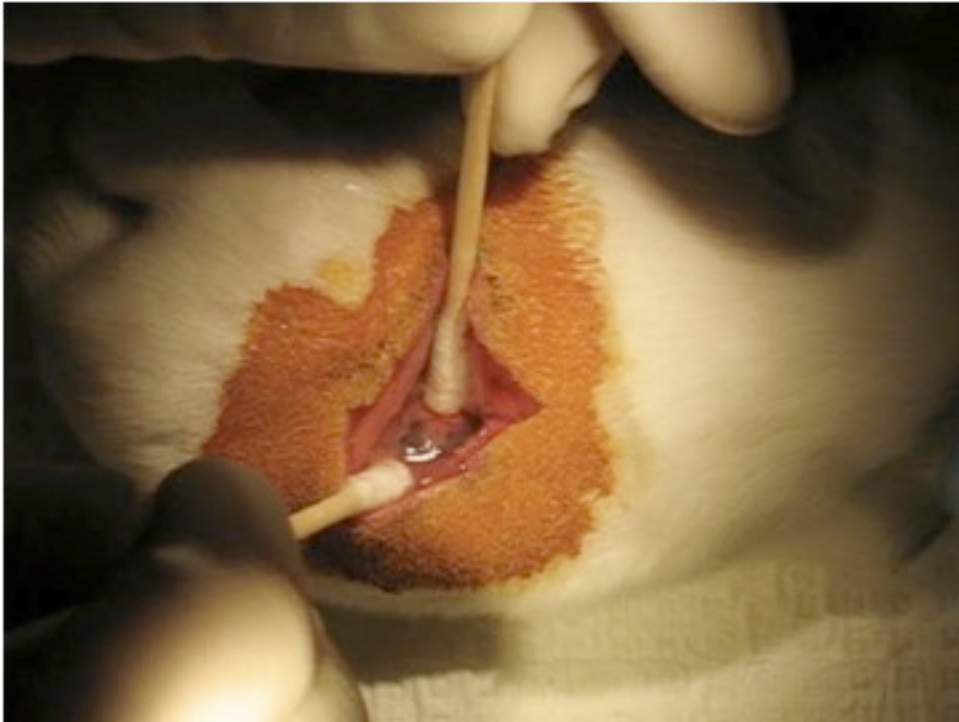


Figure 2.1 - Representative picture of a retroperitoneal incision performed on a 7 day-old rabbit. The retroperitoneal incision is performed to expose the sub-renal portions of the aorta and the inferior vena cava (IVC).

Figure 2.2

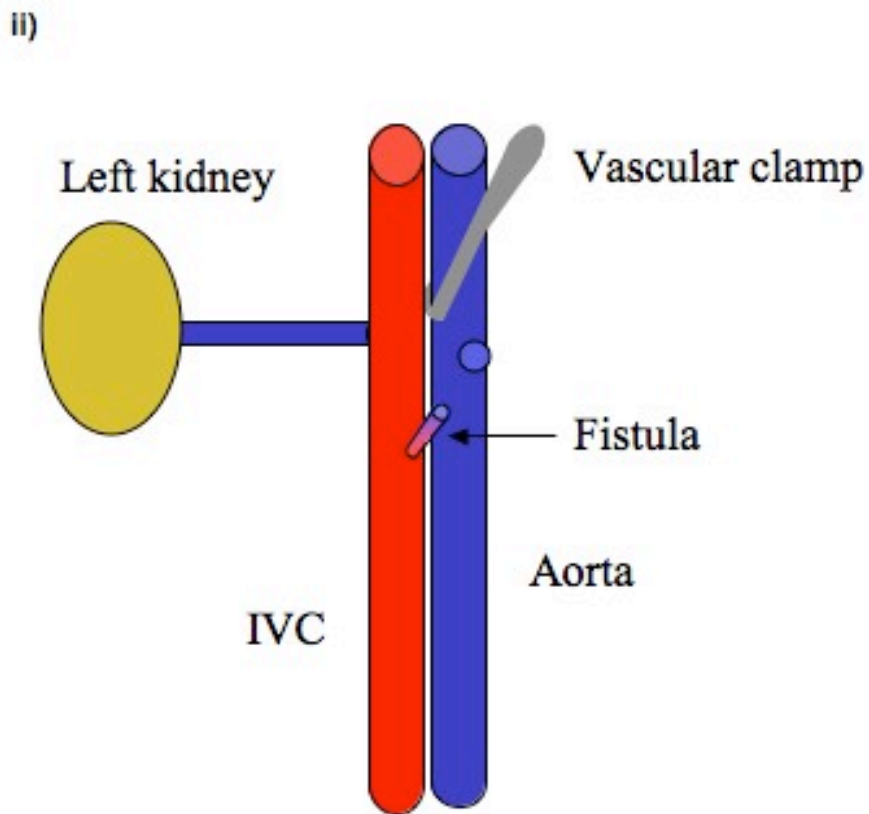
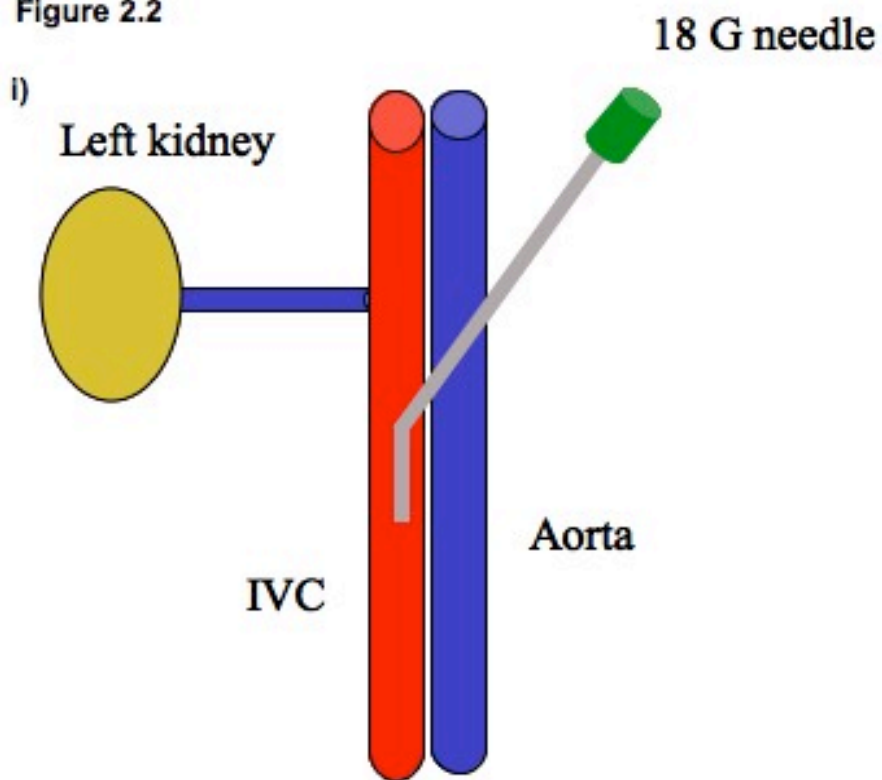


Figure 2.2 - Aorta-caval fistula. Schematic of the procedure performed to produce an aorta-caval fistula on a 7 day-old rabbit. The 18 G needle used is modified with a 45° at the edge to facilitate puncture. The aorta is first punctured followed by a through and through puncture all the way to the lumen of the IVC (i). Following puncture the aorta is clamped and the needle removed. A drop of cyanoacrylate glue is placed over the aortic puncture site (ii). After the glue is dry the clamp is removed and the incision sutured. A patent fistula is a leakage point between the arterial and venous circulations. Since the mean pressure of the arterial circulation is higher than that of the venous circulation, a patent fistula allows leakage of blood from the arterial circulation to the venous circulation.

Figure 2.3

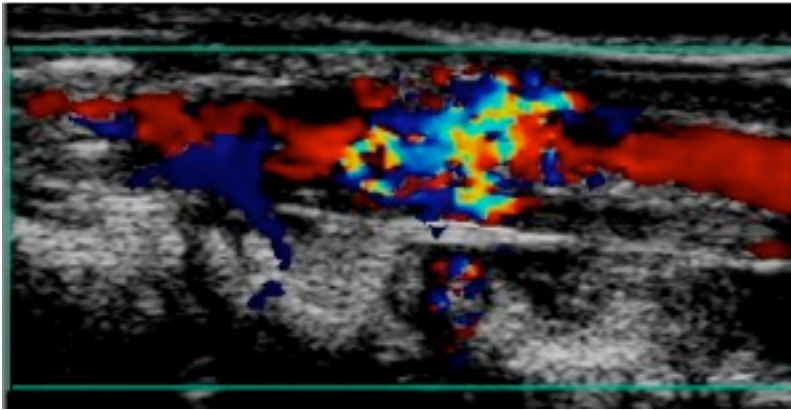


Figure 2.3 - Color Doppler. Representative frame of shunt flow viewed by color Doppler. The red color represents positive flow or flow towards the transducer (aortic flow). The blue color represents flow away from the transducer (IVC flow). The mosaic pattern is representative of turbulent flow, in this case the presence of a fistula between the IVC and the aorta

Figure 2.4

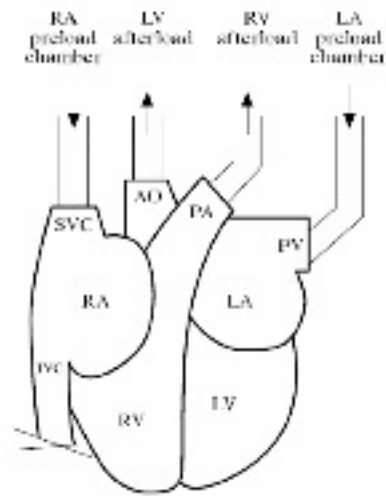


Figure 2.0.4 - The isolated biventricular heart. Schematic of the isolated biventricular working heart. The aorta is first cannulated and reversely perfused to maintain coronary perfusion. The pulmonary artery (PA) is then isolated and cannulated, followed by the superior vena cava (SVC). The inferior vena cava (IVC) is isolated and clamped. Finally, the left atrium is cannulated. (From Itoi and Lopaschuk 1993).

Figure 2.5

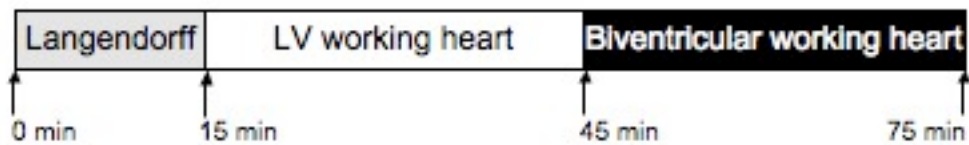


Figure 2.0.5 - Schematic representation of the perfusion protocol for the isolated biventricular working heart perfusions. During an initial period of stabilization in a retrograde Langendorff perfusion the pulmonary artery, superior vena cava and the pulmonary veins were isolated and cannulated. The inferior vena cava was isolated and occluded. After 15 minutes of Langendorff perfusion flow into the left atria was initiated and isolated left ventricular working heart perfusion performed for 30 min. After 30 min biventricular perfusion was started

by allowing flow through the cannula into the right atria through the superior vena cava. Biventricular perfusion was maintained for 30 min.

3. Results

Pre-load curves

The previous study using an isolated biventricular working heart model was performed on 14 day-old rabbit hearts (Itoi and Lopaschuk 1993). Since we were using 21 day-old rabbit hearts we performed pre-load curves to optimize the pre-loads for both the right and the left ventricle.

Figure 3.1 represents the results obtained for cardiac work for control, sham and shunt hearts. In control hearts the consecutive increase in LV pre-load or RV pre-load did not change cardiac work (Figure 3.1 A). Increasing RV pre-load at a constant LV pre-load resulted in increasing right ventricular cardiac work. With these results in mind sham hearts were subjected to a similar protocol (Figure 3.1 B). Left ventricular work was similar despite the pre-load. However, when right ventricular load was added LV work decreased considerably (43 ± 2 vs. 32 ± 4). Nonetheless, right ventricular work was stable and comparable to control values (Sham 6.1 ± 1.9 vs. Control 5.72 ± 0.54). Shunt operated hearts performed similarly to sham and control hearts at the various pre-loads (Figure 3.1 C). More importantly, at a left ventricular pre-load of 13.5 mmHg and a right ventricular pre-load of 12.5 mmHg cardiac work was 39 ± 11 and 4.8 ± 2.6 mmHg.ml/min/100, respectively. Based on these results we opted to use 11 and 12 mmHg for right and left ventricular pre-loads, respectively.

Cardiac physiology alterations due to an aorta-caval shunt

As predicted, the presence of an aorta-caval fistula results in the development of cardiac hypertrophy. This increase is observed not only in the right ventricle dimensions but it also affects the left ventricle morphology. A dramatic increase in ventricular dimensions is observed, namely right ventricle area (RVA). In hypertrophic hearts from the shunt group, RVA increases more than 31% in comparison to the non-hypertrophic hearts from the sham group. The effect of a right ventricular volume overload-induced hypertrophy on the left heart was evaluated by changes in the end diastolic volume of the left ventricle (LVEDV). In fact, LVEDV increased from 8.59 mm³ in the sham hearts to 9.76 mm³ in the shunt hearts, which represents an increase of more than 13% ($p < 0.05$). The presence of an aorta-caval fistula results in an increased flow from the aorta to the inferior vena cava. This can be detected by color Doppler as shown previously in figure 2.3. This increased flow to the inferior vena cava results in a consequent increase of its diameter. As a consequence of the presence of an aorta-caval fistula, IVC diameter increased more than 38% in hypertrophic hearts, in comparison to sham hearts.

Biventricular working heart perfusions

Two weeks after surgery hearts were excised and perfused according to the protocol described in the Methods section. Throughout the perfusion

functional data was acquired and recorded in order to evaluate functional performance. Table 2 summarizes the data obtained throughout the perfusion protocol for both groups in the two different perfusion conditions.

Of the seven parameters measured throughout the perfusion and the 3 calculated parameters (left ventricular cardiac work - LV CW, right ventricular cardiac work - RV CW and coronary flow - CF) in only one of these (heart rate) there was a difference between the groups. In fact, the heart rate of a hypertrophic shunt heart with right ventricle load added is significantly lower in comparison to the sham hearts (238 ± 0.98 vs. 265 ± 2.6 bpm, $p < 0.05$). The addition of right ventricular load results in an increase in heart rate in both groups (10% in the sham group and 7% in the shunt group). This increase is statistically significant in the sham group (Univentricular 239 ± 5.0 vs. Biventricular 265 ± 2.6 bpm, $p < 0.05$).

As a consequence of the addition of right ventricular load, both left ventricular peak systolic pressure (LV PSP) and aortic flow (AF) decreased, which is an indicator of a likely increase in the resistance of the septum wall. Left ventricular PSP significantly decreases by 11% in both groups. This decrease is accompanied by a dramatic decrease of 34% in AF in the sham group (Uni 36.3 ± 1.6 vs. Biv 23.8 ± 2.5 ml). Although a 20% decrease was seen on average on the AF in the shunt group, these failed to reach statistical significance ($p > 0.05$).

One common parameter used to evaluate heart function in a perfusion apparatus is LV CW, which is the product of LV PSP by CO. In the sham group LV CW significantly decreased in the biventricular setting, in comparison with

the univentricular setting (Uni 39.15 ± 1.02 vs. Biv 28.70 ± 2.04 mmHg.ml/min/100, $p < 0.05$). LV CW for shunt hearts did not change with the addition of right ventricular load and were not significantly different from the correspondent sham groups.

Similar parameters can be used in a biventricular setting to evaluate right heart function. Right ventricular PSP did not change between groups. The addition of right ventricular load to the working hearts did not result in any change in the developed systolic pressure. With the beginning of a biventricular perfusion flow through the superior vena cava (SVC) begins. Flow through the SVC (SVCF) was not different between the groups. As with LV CW, right ventricular cardiac work (RV CW) can be determined as the product of RV PSP by SVCF. Right ventricular CW was similar between groups. As a consequence of RV work, pulmonary artery flow (PAF) increases dramatically in both groups (Sham Uni 18.07 ± 0.29 vs. Biv 52.07 ± 0.76 ml/min; Shunt Uni 20.50 ± 0.75 vs. Biv 59.17 ± 0.89 ml/min, $p < 0.05$ vs. Uni).

Coronary flow (CF) was similar in both groups for each of the perfusion apparatus.

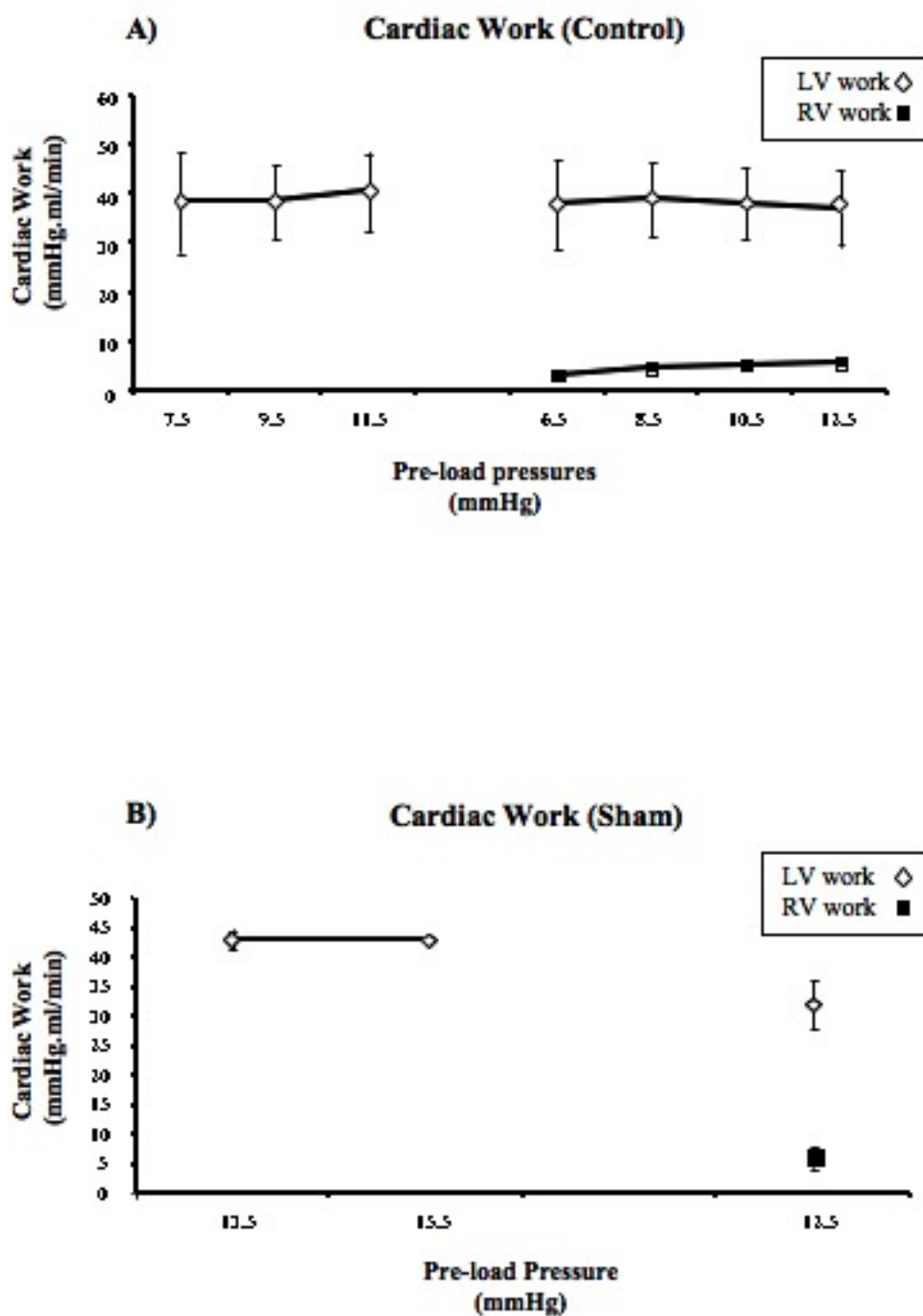
Steady state metabolic rates were determined for palmitate (0.8 mM) and glucose (5.5 mM) (undergoing oxidation or glycolytic metabolism). Steady state palmitate oxidation rates did not change between univentricular and biventricular perfusion for any of the groups (Figure 3.2 A)). However, for both univentricular and biventricular perfusions, POx rates were significantly lower in the shunt group in comparison to the sham group (Shunt Univentricular 232 ± 45 and

Biventricular 278 ± 40 vs. Sham Univentricular 583 ± 54 and Biventricular 579 ± 56 nmol/min/g dry, $p < 0.05$).

Addition of right ventricular load results in an increase in energy demand. In the sham hearts this increased energetic requirement is compensated by an increase in glucose oxidation rates close to 50%, from 281 ± 28 to 416 ± 44 nmol/min/g dry, $p < 0.05$ (Figure 3.2 B). In hypertrophic shunt hearts glucose oxidation rates were not different from the sham group but no significant increase in glucose oxidation rates was observed with the addition of right ventricular load (Figure 3.1 B). In hypertrophic shunt hearts, the decrease in palmitate oxidation rates observed seems to be partially compensated by an increase in glycolytic rates when compared to the sham hearts in a univentricular setting (2550 ± 362 vs. 6427 ± 675 nmol/min/g dry, $p < 0.05$ vs. sham) (Figure 3.2 C). During biventricular perfusion glycolytic rates in the shunt group are higher than in the sham group (2477 ± 351 vs. 4271 ± 355 nmol/min/g dry, $p = 0.057$ vs. sham).

Taken together these data suggest a severe deficiency in the capability of the hypertrophic hearts to produce enough energy to meet its energetic requirements. Steady state ATP production is represented in figure 3.3. It is clear the reduction in total ATP production in the shunt group, mainly due to the dramatic decrease in the contribution of palmitate oxidation to overall energy production. Nonetheless, palmitate oxidation still accounts for more than 50% of total energy production in the shunt group and close to 80% in the sham group for each of the perfusion settings (Figure 3.3 B).

Figure 3.1 - Pre-load curves



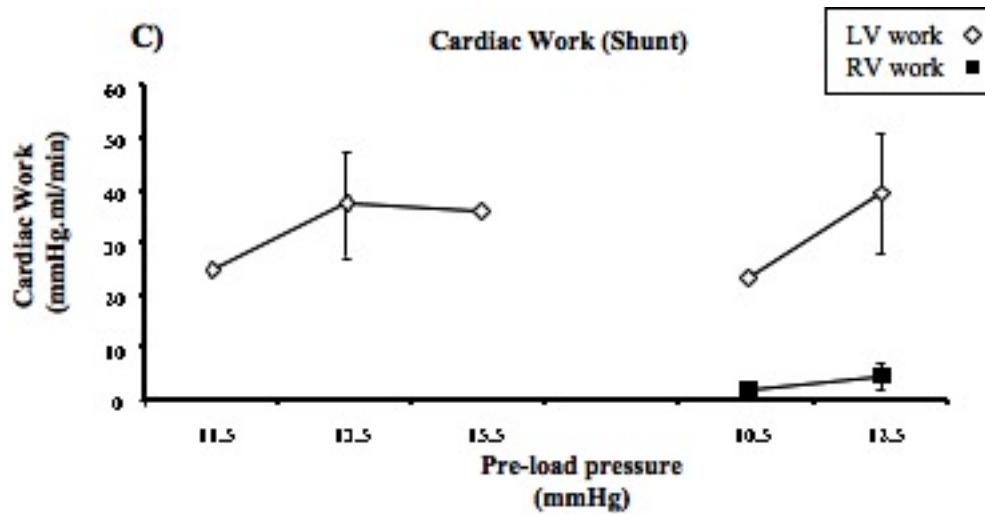


Figure 3.0.1 - Pre-load curves. In order to optimize our biventricular system in 21 day-old rabbit hearts we performed pre-load curves. To do so pre-loads to the left and right ventricle were changed independently. A) Control, n=2; B) Sham, n=2 for LV 13.5 mmHg pre-load and RV 12.5 mmHg pre-load; C) Shunt, n=3 for LV 13.5 mmHg pre-load and RV 12.5 mmHg pre-load.

Table 1 - Echocardiographic measurements. Twenty one day-old rabbits were subjected to echocardiography 2 weeks after a sham or shunt procedure. Control animals (I.e. non subjected to surgery of any type) were also used to assure that the sham procedure was not affecting cardiac physiology. LVEDV - left ventricular end-diastolic volume. * P< 0.05 shunt vs sham.

Table 1 - Echocardiographic measurements

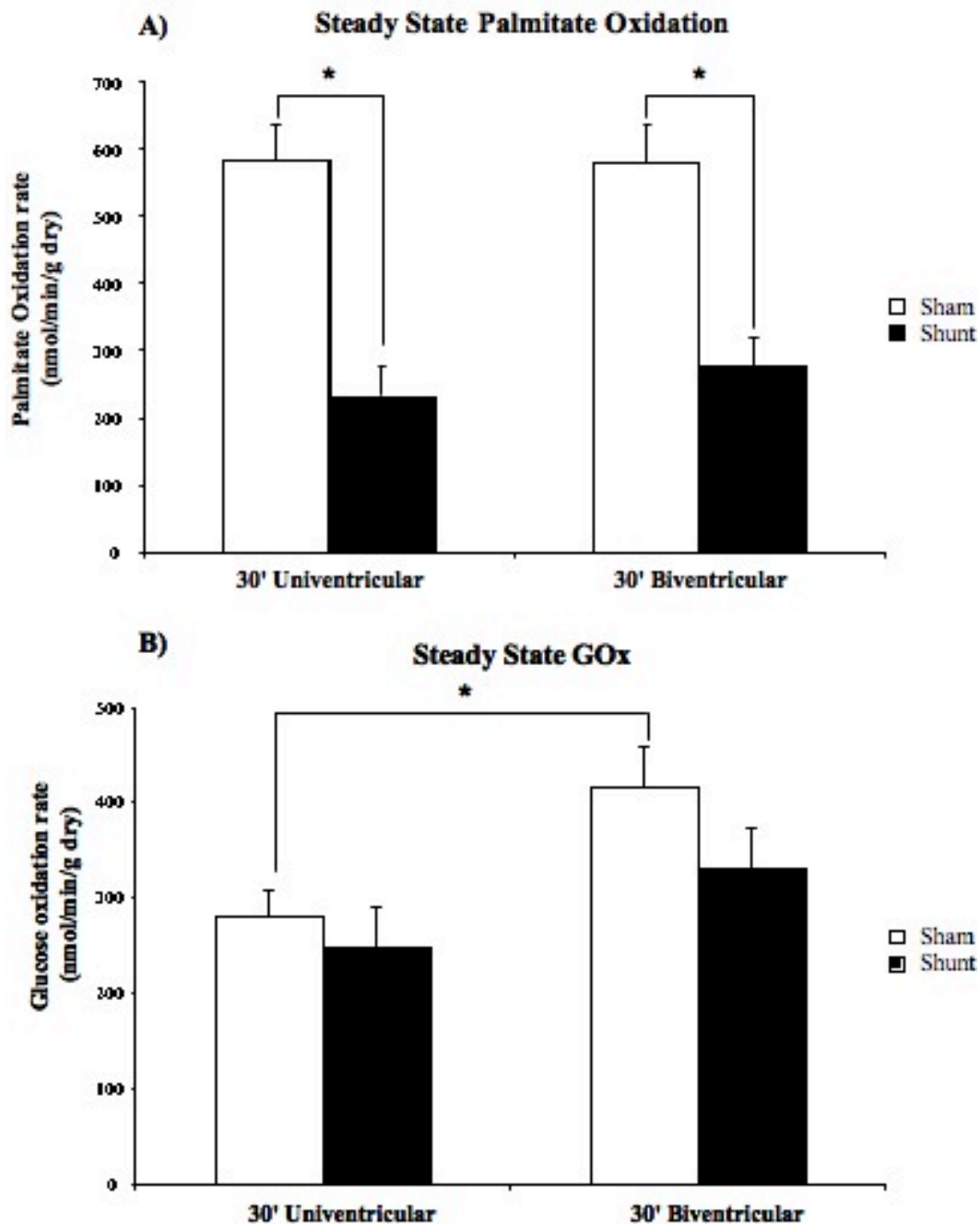
	Control	Sham	Shunt
LVEDV (mm³)	8.52 ± 0.09 (12)	8.59 ± 0.11 (12)	9.76 ± 0.13 (14) *
RV area (mm²)	30.12 ± 1.29 (7)	35.2 ± 1.96 (11)	46.33 ± 2.23 (13) *
Body Weight (g)	344.98 ± 14.49 (12)	359.57 ± 16.99 (12)	336.2 ± 15.86 (14)
IVC diameter (mm)	N/A	0.2842 ± 0.0271 (5)	0.3937 ± 0.0218 (10) *

Table 2 - Functional measurements

	HR (beats per min)	LV PSP (mmHg)	RV PSP (mmHg)	CO (ml/min)	AF (ml/min)	SVC F (ml/min)	LV CW (mmHg ml/min)	RV CW (mmHg ml/min)	PAF (ml/min)	CF (ml/min)
Sham										
Uni	2.39 ± 5.0	66.7 ± 1.0	9.0 ± 0.15	57.7 ± 0.68	36.3 ± 1.6	-	39.15 ± 1.02	-	18.07 ± 0.29	21.43 ± 1.09
Biv	2.65 ± 2.6 *	59.0 ± 1.3 *	10.2 ± 0.21	66.97 ± 2.4 *	23.8 ± 2.5 *	46.1 ± 0.44	28.70 ± 2.04 *	4.97 ± 0.15	52.07 ± 0.76 *	23.13 ± 0.21
Shunt										
Uni	2.22 ± 2.7	70.3 ± 1.4	5.6 ± 0.056	57.6 ± 0.39	40.9 ± 1.1	-	40.70 ± 1.03	-	20.50 ± 0.75	16.66 ± 0.77
Biv	2.38 ± 0.98 L	62.7 ± 1.5 *	8.01 ± 0.25	50.41 ± 2.27	32.7 ± 2.3	47.7 ± 0.33	32.10 ± 2.04	3.86 ± 0.16	59.17 ± 0.89 *	17.68 ± 0.072

Table 2 - Functional measurements. Two weeks after the shunt or sham procedure hearts were excised as described in the methods section and perfused using a biventricular perfusion apparatus. During perfusion continuous functional measurements were performed to evaluate performance mechanical performance. The average values (average of 3 replicates per heart) for each 30 minute period are shown as a measure of comparison between groups. During the first 30 minutes hearts were perfused univentricularly (Uni) followed by 30 minutes of biventricular perfusion (Biv). HR - heart rate; LV PSP - left ventricle peak systolic pressure; RV PSP - right ventricle peak systolic pressure; CO - cardiac output (measure as the flow into the heart through the left atria); AF - aortic flow; SVCF - superior vena cava flow; LV CW - left ventricular cardiac work (calculated as the product of LV PSP by CO); RV CW - right ventricular cardiac work (calculated as the product of RV PSP by SVCF); PAF - pulmonary artery flow; CF - coronary flow (calculated as the difference between CO and AF). * $p < 0.05$ vs Uni, $\perp p < 0.05$ vs Sham). Sham $n = 32$, Shunt $n = 9$.

Figure 3.2 - Steady state metabolic rates



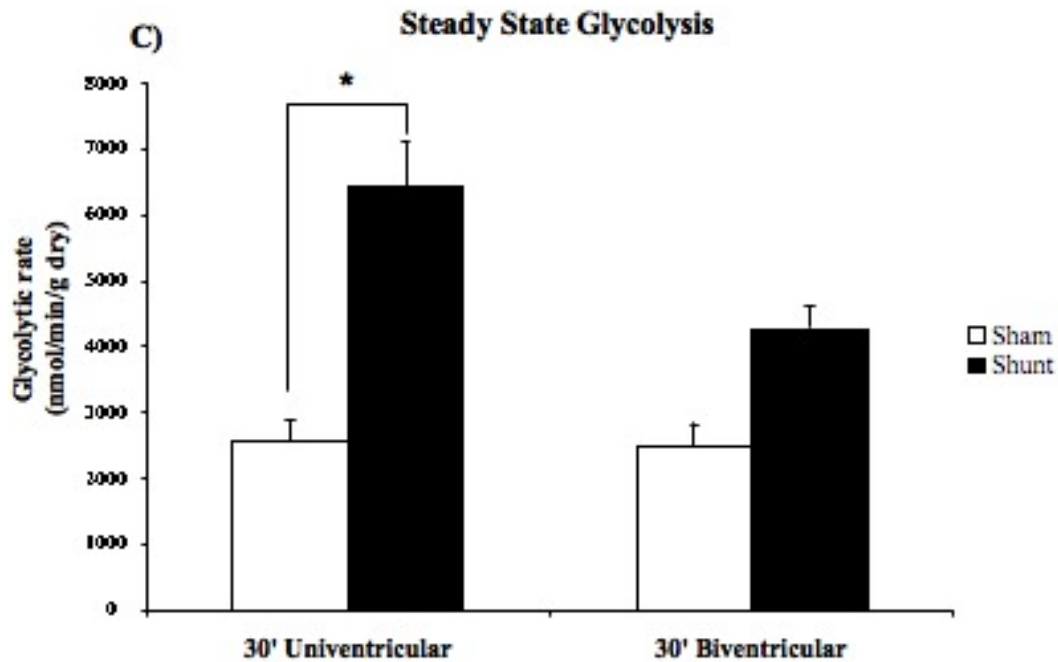


Figure 3.2 - Steady state metabolic rates. Two weeks after surgery hearts were excised and perfused. Metabolism was measured using trace amounts of radiolabeled substrates. Hearts were perfused initially for 30 minutes in a univentricular apparatus followed by 30 minutes of biventricular perfusion. Perfusion buffer contained 5.5 mM of $[5-^3\text{H}]\text{glucose}$ or $[\text{U}-^{14}\text{C}]\text{glucose}$ and $[1-^{14}\text{C}]\text{palmitate}$ and radiolabeled substrates for determination of glycolysis, glucose oxidation (GOx) and palmitate oxidation (POx) respectively. A) Steady state palmitate oxidation rates. Steady states rates do not change within a group with the addition of right ventricular load. Hypertrophic hearts from the shunt group have significantly lower POx rates for both the univentricular and the biventricular settings. This lower energetic production in the shunt group is not

compensated by an increase in GOx rates (B) but by increased glycolytic rates (C) in the univentricular system. The increased energy demand from the addition of right ventricular load is met by an increase in GOx rates in the sham but not the shunt group. * $p < 0.05$. A) sham $n = 7$, shunt $n = 5$; B) sham $n = 22$, shunt $n = 5$; C) sham $n = 35$, shunt $n = 6$.

Figure 3.3 - Steady state ATP production

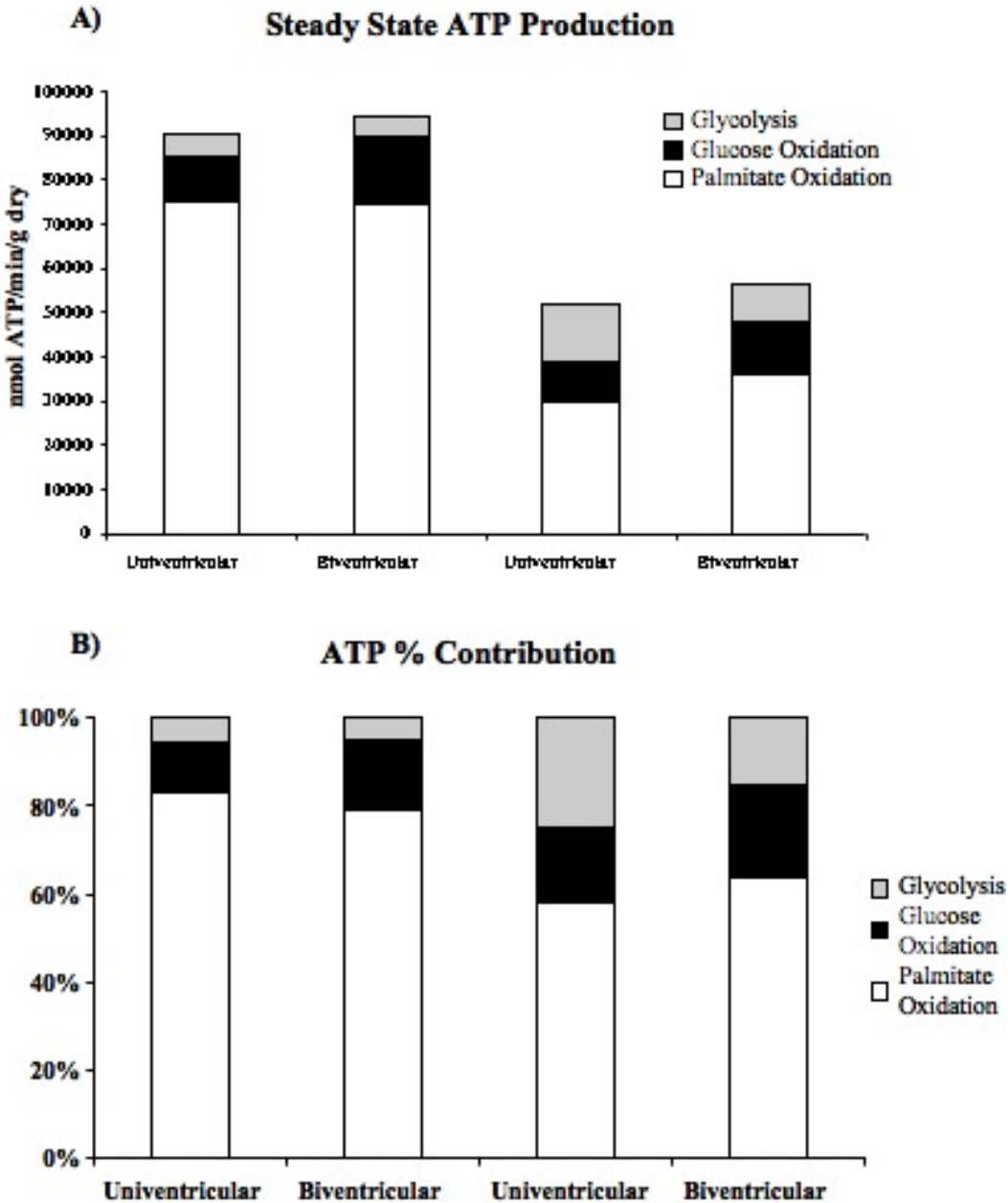


Figure 3.3 - Steady state ATP production. Each of the measured metabolic pathways contributes to overall energy production. Each palmitate molecule

undergoing beta-oxidation contributes with 129 molecules of ATP. For glucose undergoing glucose oxidation the value is 36 and undergoing glycolysis is 2. Using these considerations steady state ATP production was calculated for each group in either univentricular or biventricular perfusion (A). A percentage wise contribution to overall energy production is presented in B).

4. Discussion

The newborn heart and its energetic support are amazingly different from the adult heart. Knowing the physiological and energetic characteristics of the healthy newborn heart as well as of the hypertrophied heart is fulcrum to the proper management of cardiac function and metabolism due to neonatal heart disease. We here demonstrate the validity of using an aortocaval fistula to develop a clinically relevant newborn animal model to study volume overload hypertrophy. Furthermore, we established an isolated biventricular working heart model for 21 day-old rabbit hearts that allows the measurement of both functional and metabolic data in healthy and hypertrophied 21 day-old rabbit hearts. With these two models we determined that the increased blood return to the right ventricle results in increased ventricular dimensions two weeks after surgery. Moreover, when perfused under similar conditions, the hypertrophied hearts demonstrate a lower development of work for both left and right ventricles. These differences in function appear to be due to a decrease in energy production, namely via the fatty acid β -oxidation pathway. This decrease is accompanied by an increase in the rates of glycolysis and this fact may contribute to mechanical and energetic deficiency.

Birth marks the switch between a low and a very high circulatory demand. With birth both the lungs and the kidneys begin their full functioning in order to sustain circulatory activity. These events result in rising vascular resistance as the newborn grows. For this reason, the pre-loads and after-loads previously

described for models of isolated working heart preparations must be age specific, besides species specific. Using the setup described previously by Itoi and Lopaschuk(Itoi and Lopaschuk 1993), for an isolated biventricular working heart model in the 14 day-old rabbit heart, as a starting point we proceeded to the optimization of the system for the 21 day-old rabbit heart. While performing pre-load curve experiments one must attend that, although cardiac performance and work are vital, maintaining cardiac performance and work is equally important. We chose to use 12 mmHg as left ventricular pre-load and 11 mmHg as right ventricular pre-load. Although there was no difference in terms of cardiac work between 13.5 and 15.5 mmHg for left ventricle pre-load (figure 3.1 B and C), it was at slightly lower left ventricle pre-load that function was better maintained. The same was verified for right ventricle pre-loads. By using slightly lower loading pressures also helps us to minimize variability between experiments due to body weight changes. Although no significant differences were observed between groups in terms of body weight, the range of body weights was wide (Table 1). Differences in body weight between experiments can be attributed almost exclusively to litter size. In fact, this was a variable we were unable to control strictly. Moreover, although morbidity and mortality were under the recommended values, inter-individual variability in response to the surgical procedure could interfere with recovery of normal feeding behavior. In this study we chose to control age and not body weight. It is arguable if body weight plays a significant role in a hypertrophic heart model in comparison to age. We chose 7 day-old rabbits to undergo surgery because that was the age that would provide

higher success rate for the surgical procedure. Shunt surgeries were performed in younger rabbits (3 day-old) but the success rate of the procedure was considerably lower than in 7 day-old animals. We attribute this fact due to the high rate of cellular growth and division that results in higher tissue repair capacity of newborn animals.

The effects of volume overload produced by a fistula between the abdominal aorta and IVC was evaluated by echocardiography. It was important not only to determine if the fistula remains open after the surgery but also to achieve hypertrophic growth that is significantly higher than in sham operated animals, besides being clinically relevant. Preliminary data from our laboratory suggested that one week after surgery significant cardiac hypertrophy has developed. However, in our hands, only two weeks after surgery were we able to determine significant cardiac hypertrophic growth. Two weeks after surgery right ventricle diameter was increased by more than 50%. This increase in right ventricle dimensions is of particular importance since it is clinical relevant. In the clinical setting treatment is initiated when hypertrophy is higher than 50% (table 1). This increase in right ventricular dimensions is due to an increase circulatory return to the right ventricle. Increase blood flow to the right ventricle results in increased work demand to the ventricular muscle and hypertrophy. Of interest is the fact that left ventricle end diastolic volume was also increased. These morphological changes of the left ventricle may result from changes in compliance of the heart. Increased return to the right ventricle and increased volume on the ventricular chamber may increase the pressure on the septum

reducing its elasticity. The reduction in elasticity of the septum affects the left ventricle increasing its workload. Another explanation is due to a paracrine effect. Induction of right ventricle hypertrophy may trigger the release of paracrine mediators to the coronary circulation that induce morphological changes on the surrounding cardiomyocytes. In a model of pressure overload in juvenile rats Adrogue et al. (Adrogue, Sharma et al. 2005) demonstrated that right ventricle pressure overload induces transcriptional changes also on the left ventricle. Importantly, genes regulated by PPAR α (MCD), associated with metabolic pathways (PDK4) and the contractile machinery (myosin heavy chain β) were changed in both ventricles.

In the well described and widely used isolated working heart preparation the left heart is perfused under hemodynamic conditions close to what the hearts sees *in vivo*. In this system, the load of the left ventricle through the left atria results in the filling of the left ventricle. Stimulated by the right pre- and afterload the ventricle contracts expelling its content through the aorta. This contraction occurs with reduced tension on the septum due to absent right heart load. When right ventricle load is added, which is the case of the isolated biventricular working heart preparation, the septum is subjected to increased tension and should pose more resistance to left ventricle contraction. In fact, we here present data that is in agreement with this concept. When load was added to the right ventricle LV PSP was significantly decreased in both the sham and the shunt groups (Table 2). Since cardiac output (CO) was also significantly decreased in the sham group, LV CW was significantly lower in the sham group. Taken together these data suggest

that isolated working heart preparations, in which only left ventricular load is added to the heart, do not accurately describe the physiological status of the heart and may overestimate heart work.

Of all the hemodynamic parameters measured and calculated from isolated biventricular working heart perfusions only heart rate was significantly decreased in the biventricular perfused shunt heart in comparison to sham. The reason for this difference is not clear. Apart from heart rate all other parameters were comparable between the two groups. These results validate our choice of model and the conditions used since it allowed us to determine metabolic changes of the myocardial tissue, independent of function. Of importance is the fact that coronary perfusion is unchanged independently of uni- or biventricular perfusion and is not different between groups. This is an important observation having into account that the development of cardiac hypertrophy development due to pressure overload can result in a decrease of coronary reserve. The observed unchanged coronary flow associated with cardiac hypertrophy could result in deficient perfusion of the cardiac tissue. Moreover, right ventricular work was similar between groups. In both groups the effects of right ventricular load were similar: decreased LV PSP, and increased PA flow. The lack of significance of the decreases of CO, AF and LC CW is possibly due to the decreased number of replicates in the shunt group.

Since no difference was observed between cardiac work (right and left ventricles) in the two groups the results here described in terms of metabolic plasticity can be attributed almost exclusively to molecular adaptations on the

cardiomyocytes to volume overload of the right ventricle. Contrary to what has been previously described by Itoi and Lopaschuk (Itoi and Lopaschuk 1993), no change in palmitate oxidation rates was observed when right ventricular load was added to the heart of sham operated animals. In fact, when energy demand increases, glucose oxidation rates increase to meet the new energetic demands. It is not clear why the contradictory results between ours and those reported by Itoi and Lopaschuk. It is well accepted that during the newborn period and until weaning the major source of energy production in the heart is fatty acid β -oxidation (Ascutto, Ross-Ascutto et al. 1989; Lopaschuk, Spafford et al. 1991; Itoi and Lopaschuk 1996; Makinde, Kantor et al. 1998). This results primarily from a quick rise in circulating free fatty acids after birth together with scarce availability of carbohydrates for oxidation. Due to this very characteristic environment it has been hypothesized that glucose oxidation is immature during the newborn period and only fully matures with weaning. Our results point out in a different direction. In the 21 day-old rabbit heart, when right ventricular load is added to the heart, the increase energy demand is provided by an increase of the rates of glucose oxidation. This response of the heart to an increase in workload suggests that in the 21 day-old rabbit heart glucose oxidation is fully mature and responsive to increases in workload. The discrepancy of the results between our study and the one from Itoi and Lopaschuk can be explained from several perspectives. Firstly, the age of the rabbits used could affect the “maturation” status of the glucose oxidation pathway. The activity of the pyruvate dehydrogenase complex (PDH), which regulates the entrance of pyruvate into the

mitochondria and the TCA cycle, increases with age (Onay-Besikci, Campbell et al. 2003). A study by Abdel-aleem et al. (Abdel-aleem, St Louis et al. 1998) evaluated the effect of substrate availability on isolated cardiomyocytes from early newborn (<24h) and 2 week-old piglet hearts. Using this model the authors demonstrate that when the same mixture of physiological substrate is provided to the cardiomyocytes, the rates by which these substrates are metabolized is dependent on the age of the animal. In the early newborn period the high rates of PDH activity observed were related to high glucose, lactate and pyruvate oxidation rates in comparison to the 2 week-old piglet cardiomyocytes. These results are not in concordance with Onay-Besikci et al. and the explanation may lie in the methodology chosen. Although the model used by Onay-Besikci et al. is closer to physiological conditions – isolated working heart – the studies performed by Abdel-aleem et al. use a more physiological mixture of substrates delivered to the cardiomyocytes for oxidation, and the wide range of available carbohydrates for oxidation could be responsible for the very high activity of PDH reported. More importantly, these results seem to support the notion that at birth the heart already possesses all the machinery necessary to increase rates of glucose oxidation if demanded. In fact, when 7 day-old rabbit hearts are perfused in the absence of fatty acids glucose oxidation rates are ~1000 nmol/min/g dry wt, 5 times greater than what is observed in 1 day-old rabbit hearts perfused in the same conditions. When palmitate is added to the perfusate glucose oxidation rates decrease to ~100 nmol/min/g dry wt in both groups (Onay-Besikci, Campbell et al. 2003). These results are actually closer to what we describe here than what has

been reported by Itoi and Lopaschuk previously. Due to technical limitations at the time, the authors evaluate function as the rate between left ventricle peak systolic pressure and heart rate (rate pressure product – RPP). In our study RPP was almost double of that from 14 day-old rabbit hearts (Sham Univentricular 15.9, Biventricular 15.6 vs maximum 9.9 mmHg.bpm.10³). This difference in contractile work could explain the differences in metabolic rates. In 21 day-old rabbit hearts rates of palmitate oxidation are 10 times higher, of glucose oxidation 5 times higher and of glycolysis 4 times higher than those reported for 14 day-old rabbit hearts. Since the cocktail of substrates available for energy production are not different between the two studies, the differences in metabolic rates and consequently ATP production must be attributed to cardiac function.

The use of an aortocaval fistula is a well established model to induce cardiac hypertrophy in adult rats and pigs (Modesti, Vanni et al. 2004). Similar to what we observed in the newborn rabbits, also in adult models an aortocaval fistula results in increases in cardiac dimension, with LV and RV weight significantly increased 3 weeks after the surgical procedure. In the adult heart the development of cardiac hypertrophy, either by pressure or volume overload leads to dramatic changes of the genetic profile (Depre, Shipley et al. 1998; Kovacic, Soltys et al. 2003; Miyazaki, Oka et al. 2006). Among the many genes reported to change with adult hypertrophy are genes related to metabolic enzymes and its regulation such as pyruvate dehydrogenase kinase, fatty acid translocase/CD36, acyl-CoA oxidase and enolase, among others. It is plausible to assume that in the newborn heart the same genetic modifications occur since changes at the

proteome level have been described (Sheikh, Barrett et al. 2009). In fact, the newborn hypertrophied heart exhibits a different metabolic profile in comparison to sham hearts. When only left heart perfusion is being used, the hypertrophic heart has dramatically higher glycolytic rates in comparison to sham hearts. Increasing glucose metabolism is the most efficient way to produce energy in response to an increase in cardiac work demand, since glucose oxidation is more efficient in energy production per oxygen molecule used than fatty acid oxidation. The dramatic increase in glycolytic flux without a concomitant increase in glucose oxidation is a signal of uncoupled glucose metabolism. Uncoupling of glucose metabolism has been described as a major contributor for reperfusion injury (Neely and Grotyohann 1984). Reperfusion-induced glucose metabolism uncoupling is due to inhibition of glucose oxidation, at the level of pyruvate dehydrogenase complex, by increasing levels of acetyl-CoA produced by fatty acid β -oxidation. In our model this is not the fact. Palmitate oxidation rates are significantly lower in hypertrophied hearts in comparison to sham hearts, so inhibition of glucose oxidation by fatty acid β -oxidation cannot explain the results observed. Oka et al. (unpublished data) reported an increase in malonyl-CoA levels in left ventricles of hypertrophied newborn rabbit hearts. Malonyl-CoA is a potent endogenous inhibitor of fatty acid β -oxidation and the reported increase in its levels in hypertrophied newborn hearts may explain the observed decrease in palmitate oxidation rates observed by us. Moreover, the changes in the hypertrophied heart's metabolic profile are towards an overall reduction of oxidative metabolism. It is plausible that the observed changes of oxidative

metabolism are due to reduced availability of oxygen. In fact, unpublished data from our laboratory (Oka et al., 2010) reports an increased expression of the hypoxia-induced factor 1 α (HIF-1 α) on the right ventricle of hypertrophied newborn rabbit hearts. HIF-1 α is a transcription factor that is activated by hypoxia and suppresses oxidative phosphorylation resulting in an increase reliance on glycolysis. At the maturational level, HIF-1 α expression decreases after birth and during suckling, as the hearts reliance on glycolysis also decreases (Nau, Van Natta et al. 2002). The levels described by Oka et al. for the right ventricle of 21 day-old hypertrophic rabbit hearts are similar to those of 1 and 7 day-old rabbit hearts, leading to the indication that at the transcriptional level the newborn hypertrophic heart exhibits a switch towards the fetal profile. With increased tissue growth the demand for oxygen increases to sustain cellular function. During initial stages of hypertrophic growth angiogenesis is stimulated so that efficient perfusion of the cardiac tissue is maintained and with that, efficient delivery of oxygen is also maintained. When growth rate overcomes angiogenic rate a mismatch between delivery and demand occurs and deficient oxygen delivery seriously compromises the maintenance of oxidative metabolism. Moreover, since we observed no change in coronary flow between groups, it is plausible to argue that coronary reserve is severely decreased in hypertrophic hearts and that this is the cause to decreased oxidative metabolism. This could be the explanation why both palmitate and glucose oxidation rates are low in hypertrophied hearts and glycolysis rates are high. This incapability of the hypertrophied heart to respond to an increase in energy demand aggravates the

energy reserve problem of the newborn heart and leads to starvation of the cardiac muscle. The energy reserve problem and starvation of the cardiac muscle is evident when right heart load is added to the hypertrophied heart. When right heart load is added to the heart none of the measured energy producing pathways responds efficiently. Considering the sham heart as representing the normal physiological metabolic profile and comparing to the hypertrophied heart it is clear that the energy reserve problem hypothesized by Itoi et al (unpublished manuscript) occurs. Our results suggest that in the newborn heart metabolic rates are stimulated close to a maximum in order to meet the high energetic demand. Since the availability of carbohydrates is scarce, the newborn heart highly relies on fatty acid β -oxidation for energy production. When workload is increased and energy requirement increases (which is the case of added right heart load) the heart responds by attempting to produce more energy. With fatty acid β -oxidation rates at very high metabolic rate, glucose oxidation appears to be the chosen pathway to meet the new energetic demands. In hypertrophy, due to the reduced availability of oxygen for aerobic metabolism, the heart enters a period of energetic starvation and glycolysis is turned on to provide more energy in the form of ATP. When energetic demands are increased, in the form of increased workload, the already starved cardiac muscle is unable to efficiently stimulate energy producing pathways.

In summary, when have established the aortocaval fistula in the newborn rabbit as a valid model to induce volume overload cardiac hypertrophy. The degree of hypertrophy produced is of clinical relevance since the dimensions of

the right ventricle increased by more than 50%. Moreover, we here describe the isolated biventricular working heart preparation for 21 day-old rabbit hearts. This system allows the determination of right and left heart function *ex vivo* and evaluation of whole heart metabolism. With this system we demonstrate that in 21 day-old rabbit hearts, when right heart load is added the new energy requirements are met by an increase in glucose oxidation rates. This increased energy generation for meeting the new energetic requirements is absent in hypertrophied hearts. Hypertrophied hearts fail to stimulate energy producing pathways in response to increased workload. Moreover, when only left heart is being perfused the hypertrophied heart exhibits energetic starvation relying more on glycolysis, in comparison to the sham hearts. This information is of particular importance in the setting of surgical correction of congenital heart defects since long periods of ischemia are usually needed to perform surgery on a heart which is highly deprived of energy.

5. Future Directions

The results here reported are of extreme importance for the understanding of the energetic environment and characteristics of the newborn heart. Furthermore, these novel findings raise a number of questions concerning regulation and adaptations of the newborn heart to increased blood return due to a left to right shunt.

First, it is important to determine the molecular signaling pathway that may be involved on the metabolic changes observed in hypertrophic hearts. At the level of direct metabolic regulation the malonyl-CoA-MCD-ACC axis, together with AMPK, are top candidates to be involved in the decreased fatty acid β -oxidation observed in the shunt group. Another level of regulation may be at the transcription of enzymes involved in fatty acid metabolism. At this level estimate changes in DNA binding activity of PPARs and changes in expression of PPAR target genes may provide insight. Nonetheless, since transcription does not directly corresponds to expression or activity of a protein, a proteomics approach could be helpful in determining other proteins possibly involved in the metabolic profile exhibited by the newborn hypertrophic heart.

Also of interest would be to determine the regulatory pathways involved in the different metabolic profiles exhibited by the ventricles of the newborn heart. It is not clear why, when right ventricular work is added to the isolated newborn rabbit heart, the extra energy requirement is met by an increase in glucose oxidation. Changes in protein content between right and left ventricle

have been observed and this could help explain the changes observed in terms of metabolic rates. A protein profiling of both ventricles, targeting protein involved in metabolism regulation and metabolic pathways should be performed in order to elucidate the causes for the different metabolic profiles of the right and left ventricles.

6. Limitations

The model adopted by us to determine the consequences of cardiac hypertrophy on newborn heart metabolism can be subject of discussion. Although the presence of a fistula between the systemic and venous circulation can reproduce a physiologically relevant volume overload hypertrophy model, the age at which the surgery is performed can be subject to discussion. Surgery was performed on 7 day-old rabbits due to size limitations. At this time it is expected that the ductus arteriosus is close, being this the last physiological circulatory shunt to close. Inducing hypertrophy at 7 days of age may not mimic completely the pathological clinical scenarios on the human newborn heart. It is our belief, however, that the surgery is done at an early enough time to achieve clinical relevance.

The perfusion model adopted by us allows for a better characterization of cardiac metabolism in comparison to the isolated working heart. We used palmitate as the only substrate for fatty acid oxidation. This is a limitation to the evaluation of the real contribution of fatty acid β -oxidation to overall cardiac energy production. Sheikh et al demonstrated that due to hypertrophy there is an increase in enzymes related to medium-chain fatty acid β -oxidation. It is possible that the hypertrophied heart switches from long-chain fatty acids to medium-chain fatty acids as a primary substrate for β -oxidation. This switch in the preferred substrate for fatty acid β -oxidation cannot be determined by our perfusion system. Moreover, it has been reported that anapleurotic supply of the tricarboxylic cycle

by pyruvate can contribute up to 15% of overall energy production. In our perfusions we did not provide pyruvate nor we measured the contribution of pyruvate to energy production. It is plausible to believe that in times of energy deprivation anapleurotic contribution to overall energy production might be increased.

The results here reported are hence to be taken into account with a certain degree of limitation since not all the possible energy producing pathways were evaluated in terms of their contribution to overall energy production. Furthermore, the possibility that the surgical procedure does not accurately describe the pathological development in the newborn heart must be taken into account.

Bibliography

- Abdel-aleem, S., J. St Louis, et al. (1998). "Regulation of carbohydrate and fatty acid utilization by L-carnitine during cardiac development and hypoxia." Mol Cell Biochem **180**(1-2): 95-103.
- Adrogoe, J. V., S. Sharma, et al. (2005). "Acclimatization to chronic hypobaric hypoxia is associated with a differential transcriptional profile between the right and left ventricle." Mol Cell Biochem **278**(1-2): 71-8.
- Aitman, T. J., A. M. Glazier, et al. (1999). "Identification of Cd36 (Fat) as an insulin-resistance gene causing defective fatty acid and glucose metabolism in hypertensive rats." Nat Genet **21**(1): 76-83.
- Allard, M. F., B. O. Schonekess, et al. (1994). "Contribution of oxidative metabolism and glycolysis to ATP production in hypertrophied hearts." Am J Physiol **267**(2 Pt 2): H742-50.
- Allard, M. F., R. B. Wambolt, et al. (2000). "Hypertrophied rat hearts are less responsive to the metabolic and functional effects of insulin." Am J Physiol Endocrinol Metab **279**(3): E487-93.
- Ascutto, R. J., N. T. Ross-Ascutto, et al. (1989). "Ventricular function and fatty acid metabolism in neonatal piglet heart." Am J Physiol **256**(1 Pt 2): H9-15.
- Bache, R. J. (1988). "Effects of hypertrophy on the coronary circulation." Prog Cardiovasc Dis **30**(6): 403-40.
- Burns, K. A. and J. P. Vanden Heuvel (2007). "Modulation of PPAR activity via phosphorylation." Biochim Biophys Acta **1771**(8): 952-60.

- Calvani, M., E. Reda, et al. (2000). "Regulation by carnitine of myocardial fatty acid and carbohydrate metabolism under normal and pathological conditions." Basic Res Cardiol **95**(2): 75-83.
- Chien, K. R., K. U. Knowlton, et al. (1991). "Regulation of cardiac gene expression during myocardial growth and hypertrophy: molecular studies of an adaptive physiologic response." Faseb J **5**(15): 3037-46.
- Coupe, C., D. Perdereau, et al. (1990). "Lipogenic enzyme activities and mRNA in rat adipose tissue at weaning." Am J Physiol **258**(1 Pt 1): E126-33.
- Depre, C., G. L. Shipley, et al. (1998). "Unloaded heart in vivo replicates fetal gene expression of cardiac hypertrophy." Nat Med **4**(11): 1269-75.
- Diradourian, C., J. Girard, et al. (2005). "Phosphorylation of PPARs: from molecular characterization to physiological relevance." Biochimie **87**(1): 33-8.
- Duee, P. H., J. P. Pegorier, et al. (1985). "Hepatic triglyceride hydrolysis and development of ketogenesis in rabbits." Am J Physiol **249**(5 Pt 1): E478-84.
- Dyck, J. R., A. J. Barr, et al. (1998). "Characterization of cardiac malonyl-CoA decarboxylase and its putative role in regulating fatty acid oxidation." Am J Physiol **275**(6 Pt 2): H2122-9.
- Esposito, G., A. Rapacciuolo, et al. (2002). "Genetic alterations that inhibit in vivo pressure-overload hypertrophy prevent cardiac dysfunction despite increased wall stress." Circulation **105**(1): 85-92.

- Gamble, J. and G. D. Lopaschuk (1997). "Insulin inhibition of 5' adenosine monophosphate-activated protein kinase in the heart results in activation of acetyl coenzyme A carboxylase and inhibition of fatty acid oxidation." Metabolism **46**(11): 1270-4.
- Girard, J., P. Ferre, et al. (1992). "Adaptations of glucose and fatty acid metabolism during perinatal period and suckling-weaning transition." Physiol Rev **72**(2): 507-62.
- Hardie, D. G. and D. Carling (1997). "The AMP-activated protein kinase--fuel gauge of the mammalian cell?" Eur J Biochem **246**(2): 259-73.
- Hardie, D. G. and K. Sakamoto (2006). "AMPK: a key sensor of fuel and energy status in skeletal muscle." Physiology (Bethesda) **21**: 48-60.
- Heineke, J. and J. D. Molkentin (2006). "Regulation of cardiac hypertrophy by intracellular signalling pathways." Nat Rev Mol Cell Biol **7**(8): 589-600.
- Hoffman, J. I. (1995). "Incidence of congenital heart disease: I. Postnatal incidence." Pediatr Cardiol **16**(3): 103-13.
- Hoffman, J. I. (1995). "Incidence of congenital heart disease: II. Prenatal incidence." Pediatr Cardiol **16**(4): 155-65.
- Iemitsu, M., T. Miyauchi, et al. (2001). "Physiological and pathological cardiac hypertrophy induce different molecular phenotypes in the rat." Am J Physiol Regul Integr Comp Physiol **281**(6): R2029-36.
- Isoyama, S., N. Ito, et al. (1989). "Complete reversibility of physiological coronary vascular abnormalities in hypertrophied hearts produced by pressure overload in the rat." J Clin Invest **84**(1): 288-94.

- Itoi, T., L. Huang, et al. (1993). "Glucose use in neonatal rabbit hearts reperfused after global ischemia." Am J Physiol **265**(2 Pt 2): H427-33.
- Itoi, T. and G. D. Lopaschuk (1993). "The contribution of glycolysis, glucose oxidation, lactate oxidation, and fatty acid oxidation to ATP production in isolated biventricular working hearts from 2-week-old rabbits." Pediatr Res **34**(6): 735-41.
- Itoi, T. and G. D. Lopaschuk (1996). "Calcium improves mechanical function and carbohydrate metabolism following ischemia in isolated Bi-ventricular working hearts from immature rabbits." J Mol Cell Cardiol **28**(7): 1501-14.
- Kantor, P. F., M. A. Robertson, et al. (1999). "Volume overload hypertrophy of the newborn heart slows the maturation of enzymes involved in the regulation of fatty acid metabolism." J Am Coll Cardiol **33**(6): 1724-34.
- Kovacic, S., C. L. Soltys, et al. (2003). "Akt activity negatively regulates phosphorylation of AMP-activated protein kinase in the heart." J Biol Chem **278**(41): 39422-7.
- Krenz, M. and J. Robbins (2004). "Impact of beta-myosin heavy chain expression on cardiac function during stress." J Am Coll Cardiol **44**(12): 2390-7.
- Lauschke, J. and B. Maisch (2009). "Athlete's heart or hypertrophic cardiomyopathy?" Clin Res Cardiol **98**(2): 80-8.
- Lopaschuk, G. D. and M. A. Spafford (1990). "Energy substrate utilization by isolated working hearts from newborn rabbits." Am J Physiol **258**(5 Pt 2): H1274-80.

- Lopaschuk, G. D., M. A. Spafford, et al. (1991). "Glycolysis is predominant source of myocardial ATP production immediately after birth." Am J Physiol **261**(6 Pt 2): H1698-705.
- Lopaschuk, G. D., L. A. Witters, et al. (1994). "Acetyl-CoA carboxylase involvement in the rapid maturation of fatty acid oxidation in the newborn rabbit heart." J Biol Chem **269**(41): 25871-8.
- Lorell, B. H. and W. Grossman (1987). "Cardiac hypertrophy: the consequences for diastole." J Am Coll Cardiol **9**(5): 1189-93.
- Makinde, A. O., P. F. Kantor, et al. (1998). "Maturation of fatty acid and carbohydrate metabolism in the newborn heart." Mol Cell Biochem **188**(1-2): 49-56.
- Mandard, S., M. Muller, et al. (2004). "Peroxisome proliferator-activated receptor alpha target genes." Cell Mol Life Sci **61**(4): 393-416.
- Mandard, S., F. Zandbergen, et al. (2004). "The direct peroxisome proliferator-activated receptor target fasting-induced adipose factor (FIAF/PGAR/ANGPTL4) is present in blood plasma as a truncated protein that is increased by fenofibrate treatment." J Biol Chem **279**(33): 34411-20.
- Miyazaki, H., N. Oka, et al. (2006). "Comparison of gene expression profiling in pressure and volume overload-induced myocardial hypertrophies in rats." Hypertens Res **29**(12): 1029-45.

- Modesti, P. A., S. Vanni, et al. (2004). "Different growth factor activation in the right and left ventricles in experimental volume overload." Hypertension **43**(1): 101-8.
- Nau, P. N., T. Van Natta, et al. (2002). "Metabolic adaptation of the fetal and postnatal ovine heart: regulatory role of hypoxia-inducible factors and nuclear respiratory factor-1." Pediatr Res **52**(2): 269-78.
- Neely, J. R. and L. W. Grotyohann (1984). "Role of glycolytic products in damage to ischemic myocardium. Dissociation of adenosine triphosphate levels and recovery of function of reperfused ischemic hearts." Circ Res **55**(6): 816-24.
- Onay-Besikci, A., F. M. Campbell, et al. (2003). "Relative importance of malonyl CoA and carnitine in maturation of fatty acid oxidation in newborn rabbit heart." Am J Physiol Heart Circ Physiol **284**(1): H283-9.
- Opie, L. H., P. J. Commerford, et al. (2006). "Controversies in ventricular remodelling." Lancet **367**(9507): 356-67.
- Porrello, E. R., R. E. Widdop, et al. (2008). "Early origins of cardiac hypertrophy: does cardiomyocyte attrition programme for pathological 'catch-up' growth of the heart?" Clin Exp Pharmacol Physiol **35**(11): 1358-64.
- Randle, P. J., P. B. Garland, et al. (1963). "The glucose fatty-acid cycle. Its role in insulin sensitivity and the metabolic disturbances of diabetes mellitus." Lancet **1**: 785-9.
- Razeghi, P., M. E. Young, et al. (2001). "Metabolic gene expression in fetal and failing human heart." Circulation **104**(24): 2923-31.

- Rhodes, J. F., Z. M. Hijazi, et al. (2008). "Pathophysiology of congenital heart disease in the adult, part II. Simple obstructive lesions." Circulation **117**(9): 1228-37.
- Saddik, M., J. Gamble, et al. (1993). "Acetyl-CoA carboxylase regulation of fatty acid oxidation in the heart." J Biol Chem **268**(34): 25836-45.
- Sadoshima, J. and S. Izumo (1997). "The cellular and molecular response of cardiac myocytes to mechanical stress." Annu Rev Physiol **59**: 551-71.
- Sambandam, N., G. D. Lopaschuk, et al. (2002). "Energy metabolism in the hypertrophied heart." Heart Fail Rev **7**(2): 161-73.
- Schonekess, B. O., M. F. Allard, et al. (1997). "Contribution of glycogen and exogenous glucose to glucose metabolism during ischemia in the hypertrophied rat heart." Circ Res **81**(4): 540-9.
- Schonekess, B. O., M. F. Allard, et al. (1996). "Recovery of glycolysis and oxidative metabolism during postischemic reperfusion of hypertrophied rat hearts." Am J Physiol **271**(2 Pt 2): H798-805.
- Sheikh, A. M., C. Barrett, et al. (2009). "Right ventricular hypertrophy with early dysfunction: A proteomics study in a neonatal model." J Thorac Cardiovasc Surg **137**(5): 1146-53.
- Shiojima, I., K. Sato, et al. (2005). "Disruption of coordinated cardiac hypertrophy and angiogenesis contributes to the transition to heart failure." J Clin Invest **115**(8): 2108-18.

- Smeets, P. J., A. Planavila, et al. (2007). "Peroxisome proliferator-activated receptors and inflammation: take it to heart." Acta Physiol (Oxf) **191**(3): 171-88.
- Soltys, C. L., S. Kovacic, et al. (2006). "Activation of cardiac AMP-activated protein kinase by LKB1 expression or chemical hypoxia is blunted by increased Akt activity." Am J Physiol Heart Circ Physiol **290**(6): H2472-9.
- Sommer, R. J., Z. M. Hijazi, et al. (2008). "Pathophysiology of congenital heart disease in the adult: part III: Complex congenital heart disease." Circulation **117**(10): 1340-50.
- Sommer, R. J., Z. M. Hijazi, et al. (2008). "Pathophysiology of congenital heart disease in the adult: part I: Shunt lesions." Circulation **117**(8): 1090-9.
- Stanley, W. C. and M. P. Chandler (2002). "Energy metabolism in the normal and failing heart: potential for therapeutic interventions." Heart Fail Rev **7**(2): 115-30.
- Stanley, W. C., F. A. Recchia, et al. (2005). "Myocardial substrate metabolism in the normal and failing heart." Physiol Rev **85**(3): 1093-129.
- Sugden, P. H., S. J. Fuller, et al. (2008). "Glycogen synthase kinase 3 (GSK3) in the heart: a point of integration in hypertrophic signalling and a therapeutic target? A critical analysis." Br J Pharmacol **153 Suppl 1**: S137-53.
- Tanaka, T., F. Okamoto, et al. (1997). "Lack of myocardial iodine-123 15-(p-iodophenyl)-3-R,S-methylpentadecanoic acid (BMIPP) uptake and CD36

- abnormality--CD36 deficiency and hypertrophic cardiomyopathy." Jpn Circ J **61**(8): 724-5.
- Tanaka, T., K. Sohmiya, et al. (1997). "Is CD36 deficiency an etiology of hereditary hypertrophic cardiomyopathy?" J Mol Cell Cardiol **29**(1): 121-7.
- van der Vusse, G. J., M. van Bilsen, et al. (2000). "Cardiac fatty acid uptake and transport in health and disease." Cardiovasc Res **45**(2): 279-93.
- Walsh, K. (2006). "Akt signaling and growth of the heart." Circulation **113**(17): 2032-4.
- Wambolt, R. B., S. L. Henning, et al. (1999). "Glucose utilization and glycogen turnover are accelerated in hypertrophied rat hearts during severe low-flow ischemia." J Mol Cell Cardiol **31**(3): 493-502.
- Wambolt, R. B., G. D. Lopaschuk, et al. (2000). "Dichloroacetate improves postischemic function of hypertrophied rat hearts." J Am Coll Cardiol **36**(4): 1378-85.
- Wittnich, C., M. P. Belanger, et al. (2007). "Newborn hearts are at greater 'metabolic risk' during global ischemia--advantages of continuous coronary washout." Can J Cardiol **23**(3): 195-200.
- Yamazaki, T., I. Komuro, et al. (1999). "The molecular mechanism of cardiac hypertrophy and failure." Ann N Y Acad Sci **874**: 38-48.
- Young, M. E., S. Patil, et al. (2001). "Uncoupling protein 3 transcription is regulated by peroxisome proliferator-activated receptor (alpha) in the adult rodent heart." Faseb J **15**(3): 833-45.

